Received: 28 March 2022 | Accepted: 19 September 2022

DOI: 10.1111/1462-2920.16218

RESEARCH ARTICLE

environmental microbiology sfam

Summer thaw duration is a strong predictor of the soil microbiome and its response to permafrost thaw in arctic tundra

Karl J. Romanowicz | **George W. Kling**

Department of Ecology and Evolutionary Biology, University of Michigan, Ann Arbor, Michigan, USA

Correspondence
George W. Kling, Department of Ecology and Evolutionary Biology, University of Michigan, 1105 N. University Ave. Ann Arbor, MI 48109-1085, USA.
Email: gwk@umich.edu

Funding information
Division of Environmental Biology, Grant/Award Numbers: DEB-1637459, DEB-1754835; Office of Polar Programs, Grant/Award Number: OPP-1936769; U.S. Department of Energy, Grant/Award Number: DE-AC02-06CH11357

Abstract

Climate warming has increased permafrost thaw in arctic tundra and extended the duration of annual thaw (number of thaw days in summer) along soil profiles. Predicting the microbial response to permafrost thaw depends largely on knowing how increased thaw duration affects the composition of the soil microbiome. Here, we determined soil microbiome composition from the annually thawed surface active layer down through permafrost from two tundra types at each of three sites on the North Slope of Alaska, USA. Variations in soil microbial taxa were found between sites up to ~90 km apart, between tundra types, and between soil depths. Microbiome differences at a site were greatest across transitions from thawed to permafrost depths. Results from correlation analysis based on multi-decadal thaw surveys show that differences in thaw duration by depth were significantly, positively correlated with the abundance of dominant taxa in the active layer and negatively correlated with dominant taxa in the permafrost. Microbiome composition within the transition zone was statistically similar to that in the permafrost, indicating that recent decades of intermittent thaw have not yet induced a shift from permafrost to active-layer microbes. We suggest that thaw duration rather than thaw frequency has a greater impact on the composition of microbial taxa within arctic soils.

INTRODUCTION

Arctic tundra is underlain by permafrost, an ice-hardened soil layer defined by its sub-zero temperatures for two or more consecutive years (Williams & Smith, 1989). The layer of soil that lies above the permafrost undergoes annual freeze–thaw cycles and is known as the active layer. Collectively, these soils represent an important microbial ecosystem (Jansson & Tas, 2014) and a globally significant pool of sequestered carbon (Hugelius et al., 2014; Schuur et al., 2008; Tarnocai et al., 2009) that is being thawed and mobilized as climate warms (Hinzman et al., 2005; Jorgenson et al., 2006; Osterkamp & Romanovsky, 1999). Warmer soil temperatures, earlier spring thaw, and later fall freeze-up have all contributed to an increase in annual thaw depth and an extended duration of annual thaw at specific depths in tundra soil profiles (Barichivich et al., 2012; Euskirchen et al., 2006; Serreze et al., 2000). Yet, few studies have explicitly investigated how increased thaw frequency versus average thaw duration over time has affected the soil microbiome. The genomic potential of soil microbiomes determines the biotic decomposition of soil carbon and its release to the atmosphere as carbon dioxide (CO_2) and methane (CH_4) (Chen et al., 2021). Therefore, it is important to determine how increases in frequency and duration of thaw affect the composition of the soil microbiome in order to predict the microbial response to future permafrost thaw and the fate of permafrost soil carbon.

It is well established that microbiome composition varies across tundra soils (Deng et al., 2015; Frank-Fahle et al., 2014; Gittel et al., 2014; Mackelprang et al., 2011; Müller et al., 2018; Yergeau et al., 2010). In the active layer, the composition of the soil microbiome is influenced by geographic distance between sites (Malard et al., 2019) and variations in landscape topography that control dominant plant species and soil physicochemical properties (Judd et al., 2006; Judd & Kling, 2002; Taş et al., 2018; Zak & Kling, 2006). For example, geographic distance and plant species can change the regional composition of the active-layer microbiome given its direct connection with aboveground environmental conditions (Chu et al., 2011; Malard & Pearce, 2018; Romanowicz et al., 2021; Taş et al., 2018; Tripathi et al., 2018; Wallenstein et al., 2007). Additional environmental factors such as active-layer depth or soil type (Malard et al., 2019) as well as climatic variables such as temperature and precipitation (Castro et al., 2010; Nielsen & Ball, 2015) can also influence the composition of the active-layer microbiome. In permafrost, the composition of the soil microbiome is influenced by landscape age, with substantial changes in composition found along permafrost chronosequences in response to increasing age and associated stresses of the harsh permafrost environment (Mackelprang et al., 2017; Saidi-Mehrabad et al., 2020). Additional environmental factors such as ice content (Burkert et al., 2019), dispersal limitations (Bottos et al., 2018), and thermodynamic constraints imposed by prolonged freezing (Bottos et al., 2018) can influence the composition of the permafrost microbiome. What remains unclear is whether and how an increase in the frequency of thaw at depth over time, and the duration of that thaw, will affect the microbial composition of soils in the transition zone between the upper active layer and deeper permafrost.

Recent studies that attempt to predict the microbial response to permafrost thaw often focus on the microbiome composition as it exists at the time of sampling (Coolen & Orsi, 2015; Hultman et al., 2015; Mackelprang et al., 2011; Waldrop et al., 2010). Yet, over time the harsh permafrost environment can alter the composition of the microbiome by selecting for a subset of taxa originally present when the permafrost formed (Kraft et al., 2015; Liang et al., 2019; Willerslev et al., 2004). In laboratory-based incubations, these relic permafrost microbiomes have shown rapid, substantial shifts in composition within a few days of thaw (Coolen & Orsi, 2015; Mackelprang et al., 2011). The abundance of certain taxa within the relic permafrost microbiome has also been used to predict post-thaw biogeochemical rates such as methanogenesis (Waldrop et al., 2010), iron reduction (Hultman et al., 2015), and soil carbon transformations (Coolen & Orsi, 2015; Mackelprang et al., 2011). However, the results of these studies correspond weakly or not at all with multi-year in situ soil warming experiments that show little or no change in permafrost microbiome composition (Biasi et al., 2008; Lamb et al., 2011; Rinnan et al., 2007). Different outcomes between field and laboratory-based experiments are likely due to differences in the rates that temperature is manipulated. That is, field-based studies involve moderate heating of the active layer to mimic its natural extension into the permafrost, whereas laboratory-based experiments induce rapid permafrost thaw that can lead to substantial changes in the physicochemical properties of the soil and the composition of the permafrost microbiome and its associated biogeochemical functions (Mackelprang et al., 2011; Ricketts et al., 2020; Schostag et al., 2019). Here, we analyse the natural depth transition between thawed and permafrost soil microbiomes, coupled with estimates of intermittent thaw frequency and duration in this transition zone, to determine whether recent decades of intermittent freeze–thaw cycles have induced a compositional change in the relic permafrost microbiome.

Predicting microbial responses to thawing permafrost depends on how thaw frequency and thaw duration affect the depth-dependent composition of the soil microbiome. We approached these questions by assessing how the relic permafrost microbiome responds to intermittent freeze–thaw cycles in the soil transition zone between annually thawed active layer and permafrost. We combine results of thaw frequency and duration from multi-decadal thaw surveys with the genomic composition of the active layer, transition zone, and permafrost microbiomes measured at 10-cm increments along soil profiles of arctic tundra. The results demonstrate (1) how soil microbiomes differ regionally between sites located on distinct landscape ages and between distinct tundra types; (2) how active layer and permafrost microbiomes differ from each other between sites and tundra types; (3) that the transition zone microbiome remains indistinguishable from the permafrost microbiome even after decades of intermittent thaw, and (4) how thaw duration rather than intermittent thaw frequency has a greater impact on the composition of soil microbiomes at these arctic tundra sites. We propose that changes in microbiome composition across the transition from long-to-short duration thaw may be used to predict shifts in microbiome composition in response to future permafrost thaw.

EXPERIMENTAL PROCEDURES

Three sites were selected for this study on the North Slope of the Brooks Range in northern Alaska, USA (Figure 1). Sites were (1) Toolik Lake (68°37′16.18″ N, 149°36′54.17″ W); (2) Imnavait Creek (68°36′35.36″ N, 149°18′29.80″ W); and (3) Sagwon Hills (69°20′36.81″ N, 148°45′31.75″ W). Landscape age and glaciation

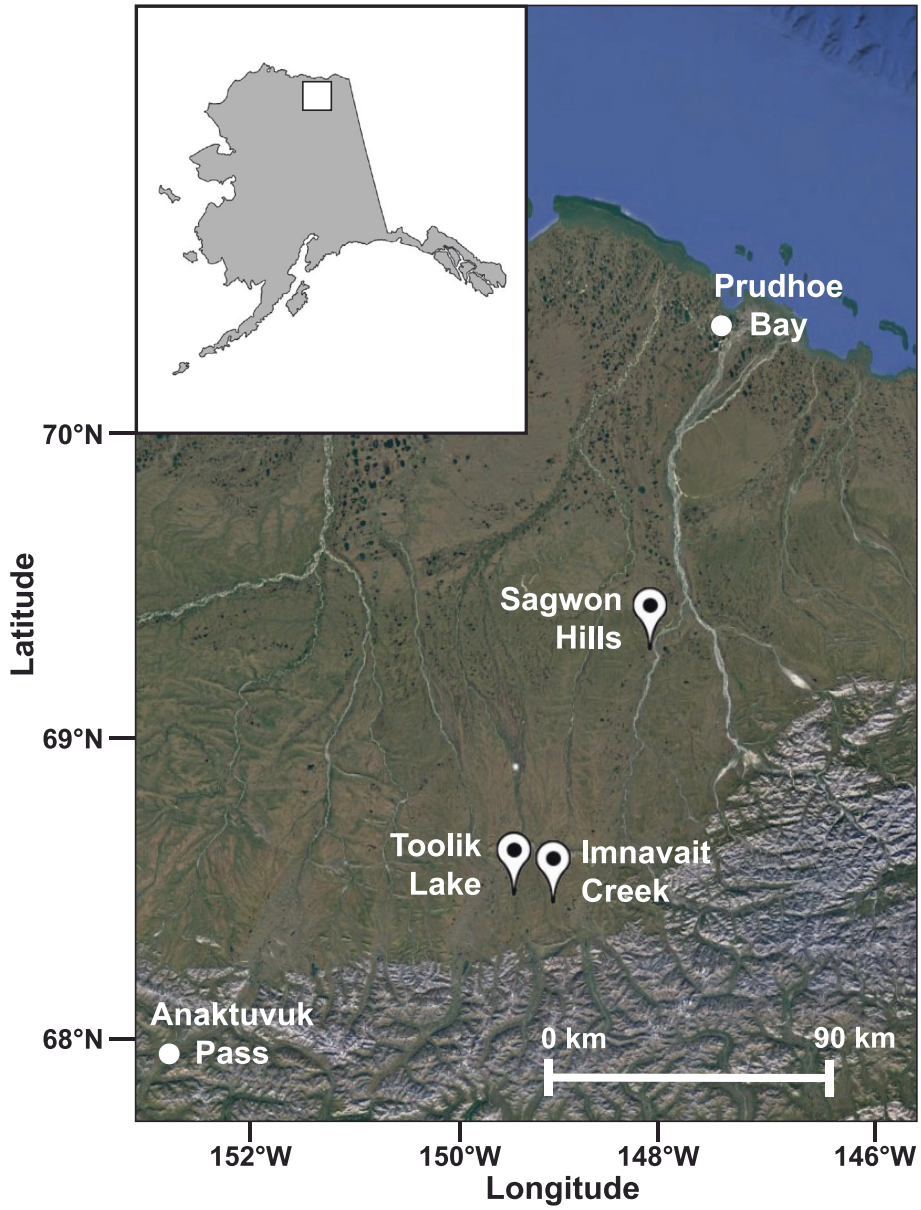

FIGURE 1 Map of sampling sites located on the north slope of the Brooks Range in northern Alaska, USA. Three study sites are (1) Toolik Lake; (2) Imnavait Creek; and (3) Sagwon Hills.

surface differed by site (see Walker et al., 2014). Briefly, soils in the Toolik Lake area formed on an Itkillik II-age landscape (~14 kyr BP), soils in the Imnavait Creek area formed on a Sagavanirktok-age landscape (~250 kyr BP), and soils in the Sagwon Hills area formed on a Gunsight Mountain-age landscape (~2500 kyr BP). Topography controlled the dominant plant species at each site such that hillslopes supported moist acidic tussock (MAT) tundra and valley bottoms supported wet sedge (WS) tundra. See Appendix S1 for additional details.

At each site, the vertical soil profile of MAT and WS tundra was sampled in 10-cm increments down to 1 m depth. Within MAT tundra, soil pits (~1 m^2 and 1 m deep) were excavated using a jack hammer, shovels, and pickaxe to expose the soil profile. Soil samples (~25 g) were collected in duplicate from each 10-cm increment along the soil profile using a chisel rinsed with 70% ethanol between depths. Samples were placed in 50 ml Falcon tubes in a cooler with ice, and immediately frozen at −80°C upon return from the field. Within WS tundra, soil cores were collected using a SIPRE (Snow, Ice, and Permafrost Research Establishment, Tarnocai, 1993) corer with carbide bits (Jon's Machine Shop, Fairbanks, AK). Soil cores were extruded then scraped parallel to soil layers using aseptic techniques in the field to remove outer layers of soil and then separated into 10-cm increments. Soil samples (~25 g) were collected in duplicate from each 10-cm increment along the soil core using a chisel

rinsed with 70% ethanol between depths. Samples were placed in 50 ml Falcon tubes in a cooler with ice, and immediately frozen at −80°C upon return from the field. Soil sampling at each site took place over the course of 1 day between 10 and 20 July 2018 for a total of 51 samples for analysis.

Annual thaw depth measurements began in 1990 at the Toolik MAT site, and in 2003 at the Imnavait MAT and WS sites. Annual thaw depth measurements have not been conducted at the Sagwon sampling location. Thaw frequency over time was characterized by calculating the probability of thaw for each 10-cm depth increment of the soil profile. This represents the probability that in any given year the surface thaw would reach that depth. Probabilities were calculated for July and August sampling dates as measured from thaw depth surveys at Toolik MAT (1990–2018), Imnavait MAT (2003–2018), and Imnavait WS (2003–2018) tundra sites. Average thaw duration (i.e. the minimum number of days the soil at a given depth was thawed) was calculated from thaw depth measurements taken at seven time points from 2 June to 20 August in 2018 at Toolik and 21 June to 21 August in 2018 at Imnavait (see also Figure S3). These are 'minimum' estimates of thaw duration because any particular depth may have thawed just after one survey but not been detected until the next survey. See Appendix S1 for additional details.

Soil physicochemical properties including soil pH, electrical conductivity (μS cm^{-1}), water content (%), and organic carbon content (%) were measured from each 10-cm soil profile increment. Bacterial cell viability assays were performed on select soil profile increments using three depths at each sampling location to represent a surface active-layer depth (~10–20 cm), a transition zone depth (~40–50 cm), and a permafrost depth (~70–80 cm). The viability assays were performed with a Live/Dead BacLight Bacterial Viability kit (Invitrogen) following methods from Burkert et al. (2019). Cell counts were corrected to calculate the average number of cells per gram of soil (dry weight). See Appendix S1 for additional details.

Genomic DNA was extracted from each 10-cm soil profile increment and amplified through polymerase chain reaction (PCR) using dual-barcoded 16S rRNA gene primers 515f-806r (Apprill et al., 2015; Parada et al., 2016) to profile the bacterial and archaeal communities. PCR amplicons were pooled into a single library and submitted to the University of Michigan Microbiome Core for high-throughput sequencing on the Illumina MiSeq platform. Sequencing data were downloaded from Illumina BaseSpace and analysed using QIIME2 (v. 2020.11) (Bolyen et al., 2019) on the Great Lakes high-performance computing cluster (University of Michigan, USA). Raw forward and reverse sequencing reads were quality filtered with DADA2 (Callahan et al., 2016). Taxonomy was assigned to amplicon sequence variants (ASVs) using scikit-learn naïve Bayes taxonomy classifier (Pedregosa et al., 2011) against the SILVA sequence database (v. 138) (Quast et al., 2012). ASVs were chosen over operational taxonomic units (OTUs) following recent benchmark studies (Callahan et al., 2016; Chiarello et al., 2022). ASVs were filtered to remove chloroplast, mitochondria, and ASVs not assigned to bacteria or archaea classification. To assess community composition along the depth profile, samples were rarefied to 50,487 sequences per sample (average 116,360 QC sequences per sample prior to rarefying), with rarefaction plots asymptotic at ~20,000 sequences for all samples. See Appendix S1 for a summary of sequencing read statistics (Table S3).

QIIME2 artefacts were exported to R (v. 4.2.1) (R Core Team, 2013) using the 'qiime2R' package (Bisanz, 2018), where all statistical analyses were conducted and considered significant at $p < 0.05$. One-way analysis of variance (ANOVA) was used to assess differences in soil physicochemical properties and microbiome alpha diversity between sites, tundra type, soil layer, and their interactions across the sampling region. Multivariate statistical analysis of the microbiome data was conducted using the 'microeco' package (Liu et al., 2021) and the 'vegan' package (Oksanen et al., 2019). Bray–Curtis dissimilarity was calculated for ASV abundance and analysed via permutational multivariate analysis of variance (PERMANOVA) using the 'adonis()' function (999 permutations) in the 'vegan' package to determine the effects of site, tundra type, and their interactions on the composition of the soil microbiome across the sampling region. Venn diagrams were generated to visualize the unique and shared ASV counts and their relative abundance between sampling sites or between tundra types. Differences in ASV abundance by individual soil depths across all sites and tundra types were visualized through unconstrained NMDS ordination using the 'metaMDS()' function in the 'vegan' package. Hierarchical clustering analysis was used to determine which soil depths were statistically similar to each other based on the vertical distribution of dominant microbial taxa, where an agglomerative clustering algorithm calculated similarity of mean z-scaled relative abundance values by soil depth and determined the optimal number of clusters from 10,000 bootstrap iterations using the 'pvclust()' function in the 'stats' package (R Core Team, 2013). Hierarchical clustering analysis was also used to determine which microbial taxa were statistically similar to each other across soil depths based on the mean z-scaled relative abundance values of each taxon at each depth, with the optimal number of clusters determined from 10,000 bootstrap iterations using the 'pvclust()' function. The hierarchical clustering results for soil depth and taxon clusters were visualized together with the 'pheatmap' package (Kolde &

Kolde, 2015). Spearman's non-parametric rank correlations (rho) were used to determine the similarity of the dominant microbial taxa (via relative abundance) with soil physicochemical properties and thaw duration measurements across all depths of the soil profile using the 'cor.test()' function. Thaw duration measurements were non-normally distributed along soil profiles and a non-parametric correlations test such as Spearman's rho was most appropriate for the data. See Appendix S1 for additional details regarding thaw frequency and duration measurements.

RESULTS AND DISCUSSION

We sampled the depth-dependent composition of the soil microbiome at 10-cm increments down soil profiles under two distinct tundra types at each of three sites separated by ~90 km on the North Slope of Alaska, USA (Figure 1). Tundra types included moist acidic tussock (MAT) tundra found on hillslopes and wet sedge (WS) tundra found in valley bottoms (see Experimental Procedures for full description). The depth-dependent distribution of microbial taxa in tundra soils has previously been investigated (Kim et al., 2016; Müller et al., 2018; Tripathi et al., 2018, 2019) and is known to be highly influenced by geographic separation between sites (biogeography) and distinct tundra types that are associated with the taxonomic composition of the active layer and permafrost microbiomes (Deng et al., 2015; Singh et al., 2017; Varsadiya et al., 2021; Wilhelm et al., 2011). Our results from high-throughput DNA sequencing analysis of bacteria and archaea are generally consistent with these previous studies by showing geographic and depth-dependent variation in microbiome composition. However, we analyse this variation in detail and relate changes in microbiome composition from the active layer through a transition zone into permafrost to the frequency and duration of intermittent thaw as determined by multi-decadal thaw surveys.

Soil microbiome diversity

For the soil microbiome analysis, 16S rRNA gene amplicons were resolved to amplicon sequence variants (ASVs) rather than operational taxonomic units (OTUs) based on recent benchmark studies comparing both sequence inference methods (Callahan et al., 2016; Chiarello et al., 2022). ASVs showed no statistical difference in taxonomic alpha diversity between sites, tundra type, or site × tundra type interactions using Chao1 and Shannon diversity metrics (ANOVA; $p > 0.05$ for all; Figure S1A,B) when all depths were included. However, there were significant depth-dependent differences in taxonomic alpha diversity between soil layers when soil depths were pooled as active layer (0–40 cm MAT tundra; 0–50 cm WS tundra) or permafrost (40+ cm MAT tundra, 50+ cm WS tundra), but only when soil layers were compared across all sampling locations (ANOVA; $p < 0.001$). There were no significant differences in alpha diversity between active layer and permafrost soil layers within any single sampling location (ANOVA; $p > 0.05$ for each). Beta diversity results based on Bray–Curtis dissimilarity of ASV abundance indicated significant differences in taxonomic composition between sites, tundra type, soil layer, and their interactions (PERMANOVA; $p < 0.001$ for all; Figure S1C). Venn diagrams indicated that the greatest relative abundance of ASVs were shared between all three sites (52.8%; Figure 2A), with an additional 25.4% of ASV abundance shared between at least two sites (Figure 2A). Notably, these ASVs represented 78.2% of the relative abundance of all ASVs shared between sites but consisted of only 4550 ASVs out of 23,798 total ASVs (Figure 2A). Likewise, the dominant ASVs shared between tundra types (69.8%; Figure 2B) consisted of only 3328 ASVs out of 23,798 total ASVs (Figure 2B). The remaining extent of ASVs were unique to each site (19,248 ASVs; Figure 2A) or each tundra type (20,470 ASVs; Figure 2B). Sagwon had the greatest abundance of unique ASVs (13.4%) compared with Toolik (4%) and Imnavait (4.3%; Figure 2A), while WS tundra had more unique ASVs (19.3%) compared with MAT tundra (10.9%; Figure 2B). Collectively, the abundance of unique ASVs by site (21.7%) or by tundra type (30.2%) suggests the potential for regional endemism consistent with previous biogeographical microbiome surveys across the Arctic (Malard et al., 2019).

Differences in ASV abundance by individual soil depths across all sites and tundra types were visualized through unconstrained non-metric multidimensional scaling (NMDS) ordination based on Bray–Curtis dissimilarity (Figure 2C). At Toolik and Imnavait sites, it appears that the relative abundance of ASVs by soil depth are strongly influenced by tundra types shared between sites rather than between tundra types within each site (Figure 2C). Notably, we found that the soil depths corresponding to MAT tundra or WS tundra overlapped between Toolik and Imnavait sites in ordination space based on their shared abundance of ASVs (Figure 2C). Beta diversity measurements also indicated no significant difference in taxonomic abundance of ASVs shared between these sites based on tundra type (PERMANOVA; $p > 0.05$ for each), while there were significant differences between tundra types within each site (PERMANOVA; $p < 0.05$ for each; Figure S1C). These results are likely due to differences in the dominant plant species known to affect soil physicochemical properties that regulate microbiome composition (Judd et al., 2006; Judd & Kling, 2002; Taş et al., 2018; Zak & Kling, 2006). For example, moist

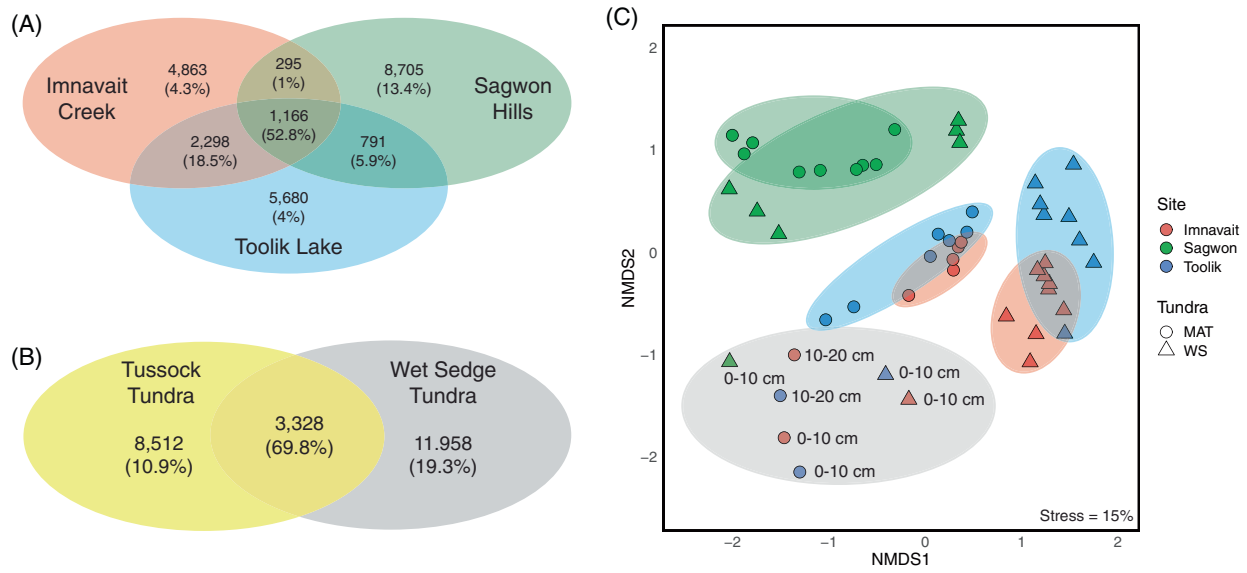

FIGURE 2 Venn diagram of unique and shared ASVs for (A) each site and (B) both tundra types. The total ASVs of each site or tundra type and those ASVs shared between sites or between tundra types are shown as counts. The relative abundance that each ASV count represents is shown as a percentage in parentheses. NMDS ordination (C) based on the Bray–Curtis dissimilarity of ASV abundance within the soil microbiome reveals regional variation by site and between tundra types. The surface depth (0–10 cm) for most sampling locations ordinated separately from all other soil profile depths (grey ellipse). Each marker represents an individual depth sampled along the soil profile of a given site by tundra type in the NMDS plot.

acidic tussock tundra is dominated by sedges (*Eriophorum vaginatum*) and dwarf shrubs (*Betula nana*, *Ledum palustre*) on hillslopes with greater soil water drainage than wet sedge tundra, which is dominated entirely by sedges (*Carex aquatilis*, *C. chordorrhiza*, *C. rotunda*) in valley bottoms where soil water accumulates (Walker et al., 1994). The ecological differences in dominant plant species between MAT and WS tundra affect soil physicochemical properties such as soil pH, water content, and the accumulation of organic C (Table S1) and likely account for the overlapping ordination of soil depths by tundra type between Toolik and Imnavait sampling locations (Figure 2C). Our results are also consistent with numerous studies showing regional variations in taxonomic abundance linked to tundra type (Chu et al., 2011; Judd et al., 2006; Tripathi et al., 2018; Wallenstein et al., 2007; Zak & Kling, 2006).

In contrast, we found overlapping ordinations for soil depths corresponding to MAT and WS tundra at Sagwon based on shared ASV abundance within the site (Figure 2C). However, there was a significant difference in taxonomic beta diversity based on the abundance of ASVs shared between tundra types at Sagwon (PERMANOVA; $p < 0.001$; Figure S1C) that may account for the distinct clustering of MAT tundra soil depths within the more dispersed cluster of WS tundra depths (Figure 2C). The Sagwon landscape is ~2500 kyr BP in age compared to the youngest landscape at Toolik (~14 kyr BP) and the intermediate-aged Imnavait (~250 kyr BP), and our sites represent a natural Pleistocene chronosequence across the sampling region (Walker et al., 2014). The greater proportion of ASVs unique to the considerably older Sagwon landscape (13.4%; Figure 2A) compared to the younger aged landscapes at Toolik and Imnavait (4%, 4.3%, respectively; Figure 2A) is also consistent with previous arctic studies showing substantial variations in taxonomic abundance by landscape age due to differences in soil physicochemical properties that develop over geologic time (Mackelprang et al., 2017; Saidi-Mehrabad et al., 2020). Here, we found that soil pH and conductivity were significantly greater at Sagwon compared to the other sites (ANOVA; $p < 0.05$; Table S1), which may account for the higher proportion of unique ASVs at Sagwon (Figure 2A) and the overlapping soil depths by tundra types within Sagwon that ordinated separately from the same tundra types shared between Toolik and Imnavait (Figure 2C). Soil pH has previously been identified as a key factor influencing the abundance of microbial taxa over both small and large geographic scales in the Arctic (Chu et al., 2010; Ganzert et al., 2014; Siciliano et al., 2014), and pH can vary by landscape age (Hultman et al., 2015; Mackelprang et al., 2017; Saidi-Mehrabad et al., 2020). Alternatively, the greater geographic distance between Sagwon and Toolik or Imnavait (~90 km; Figure 1) may have influenced microbial distribution (e.g. via dispersal limitations) across the region such that the effects of tundra type on ASV abundance by soil depths at Sagwon was minimized in our NMDS ordination (Figure 2C).

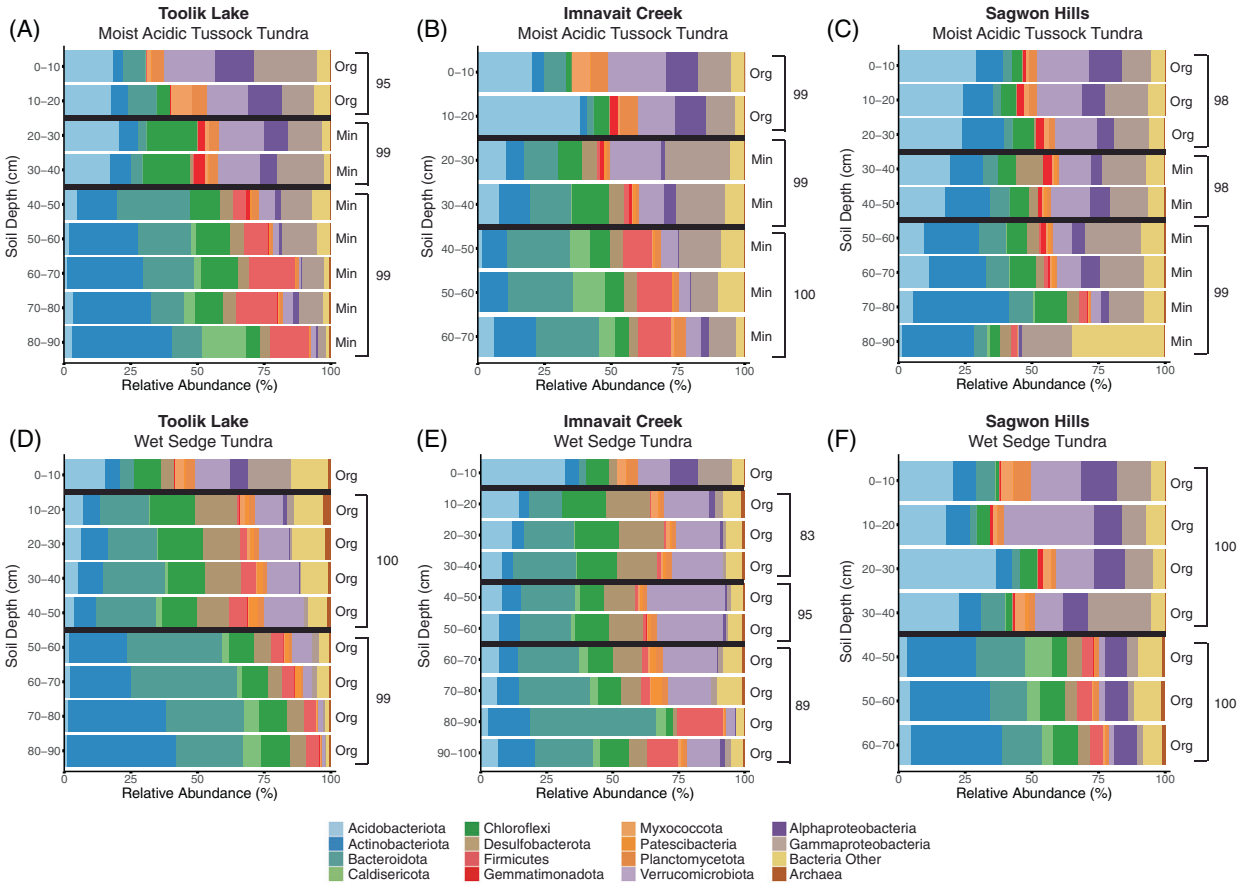

FIGURE 3 Soil microbiome composition along soil profiles within moist acidic tussock (MAT) tundra (A–C) and wet sedge (WS) tundra (D–F) for Toolik (A, D), Imnavait (B, E), and Sagwon (C, F) sampling sites. Soil pits were dug for all MAT tundra sites and soil cores were extracted from all WS tundra sites. Soil type for each sampling depth along the soil profile is indicated as 'Org' (organic) or 'Min' (mineral). Black horizontal bars delineate distinct soil layers within each soil profile as determined from the hierarchical clustering analysis, with percent similarity values (out of 100) displayed for each cluster.

All these overlapping ordination patterns of soil depths based on ASV abundance in the unconstrained NMDS plot were consistent with the relative abundance of shared and unique ASVs shown in the Venn diagrams (Figure 2A,B) and with the significant differences measured in taxonomic beta diversity (Figure S1C). Furthermore, the surface depth (0–10 cm) from five of six sampling locations (Sagwon MAT tundra as the exception) ordinated separately from all other depths within their respective soil profiles and coalesced near each other in ordination space (grey ellipse; Figure 2C). This also included the 10–20 cm surface depth for MAT tundra at Toolik and Imnavait (Figure 2C), which together indicate a unique taxonomic composition within the surface depths that is consistent across sampling locations. This strong pattern of shared taxa in surface depths across the tundra region regardless of tundra type or landscape age has not been shown before and could imply that a common dispersal mechanism such as wind is homogenizing the microbiome composition at the soil surface, and that this mechanism is strong enough to overcome the effect of differences in dominant plant species by tundra type.

Soil microbiome composition

ASV annotations, derived from the SILVA database (v. 138; Quast et al., 2012), indicated that the soil microbiome at all sampling locations with all depths combined was dominated by bacteria (>98% relative abundance). However, the relative abundance of dominant bacterial taxa changed with depth at all sampling locations (Figure 3). Using hierarchical clustering analysis on depth-dependent differences in bacterial abundance, we found that all soil profiles clustered into several distinct soil layers (Figure 4). Figure 3 delineates distinct soil layers within each soil profile with black horizontal lines between soil depths as determined from hierarchical clustering analysis (Figure 4) to visualize the depth-dependent differences in bacterial abundance along the soil profiles.

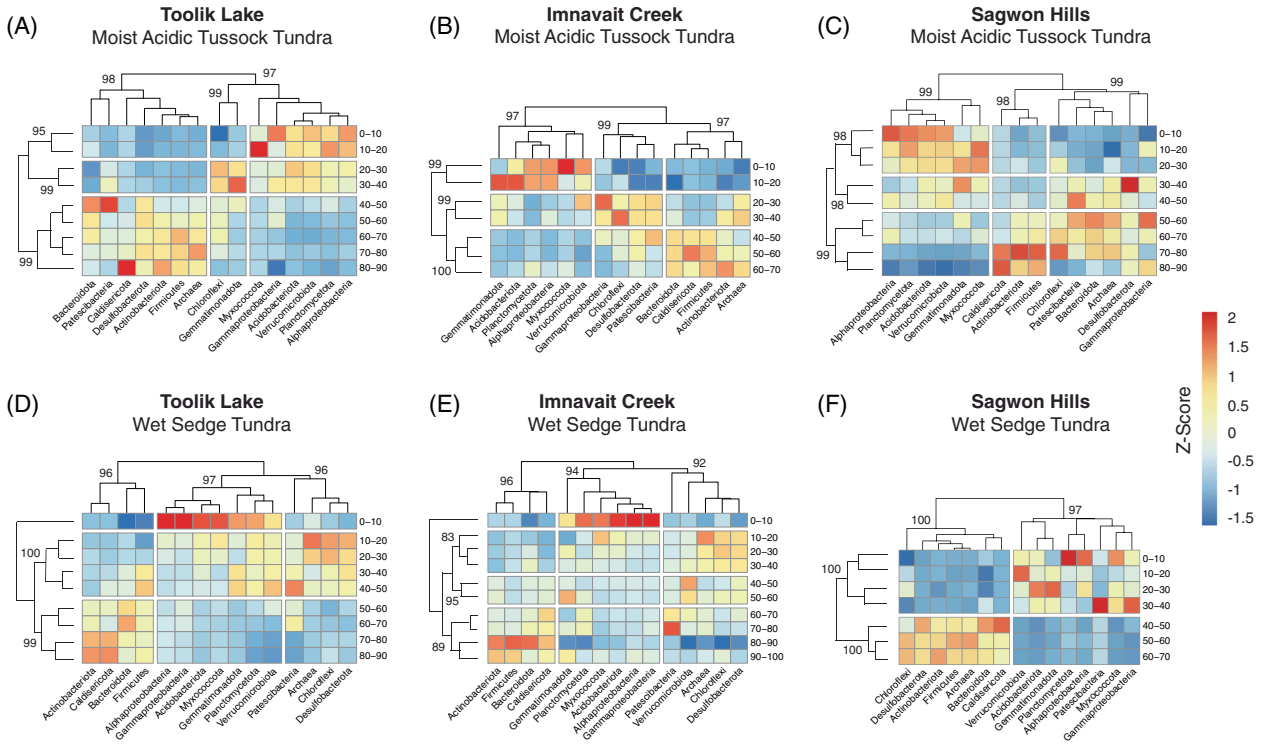

FIGURE 4 Heatmaps illustrating the significant clustering of distinct soil depths (rows) and microbial taxa (columns) for moist acidic tussock (MAT) tundra (A–C) and wet sedge (WS) tundra (D–F) at Toolik (A, D), Imnavait (B, E), and Sagwon (C, F) based on hierarchical clustering analysis. The optimal number of clusters for soil depths and microbial taxa was determined using gap statistics based on the similarity of mean z-scaled relative abundance values of microbial taxa by soil depth. The percent similarity value (out of 100) is displayed for each cluster with values greater than 95% similarity considered significant.

For Toolik and Imnavait MAT tundra, we consider the distinct soil clusters from 0 to 40 cm depth to represent the active layer, while the active layer in Sagwon MAT tundra ranged from 0 to 30 cm depth (Figure 4A–C). There was also an additional cluster of soil depths within the active layer of Toolik and Imnavait MAT tundra where the abundance of bacterial taxa clustered by different soil types (Figure 3A,B). Specifically, the surface soil depths (0–20 cm) were composed of organic soil and clustered distinctly from the lower half of the active layer (20–40 cm) that was composed of mineral soil (Figure 3A,B). Likewise, the Sagwon MAT tundra active layer (0–30 cm) was composed of organic soil that clustered distinctly from the permafrost depths (40+ cm) that were composed of mineral soil (Figure 3C). Similar results were also found in previous tundra studies where bacterial abundance was strongly related to a shift in substrate availability between the organic and mineral soil horizons (Deng et al., 2015; Koyama et al., 2014). The change from organic to mineral soil type could also account for the distinct ordination patterns of surface depth MAT tundra samples in our NMDS plot (0–10 cm, 10–20 cm; Figure 2C). The distinct cluster of bacterial taxa after 40-cm depth (30-cm Sagwon) in MAT tundra (Figure 4A–C) was not associated with a change in soil type because all soil depths below 20 cm (30-cm Sagwon) were composed of mineral soil (Figure 3A–C). Thus, the distinct cluster after 40-cm depth (30-cm Sagwon) likely indicates the average permafrost boundary (described below).

In contrast, the WS tundra soil profiles were composed entirely of organic soil (Figure 3D–F); thus, the clustering patterns of shared bacterial taxa into distinct soil layers are not due to major changes in soil type with depth (Figure 4D–F). Rather, these clustering patterns are likely due to the substantial differences in taxonomic abundance at the surface-most depth (0–10 cm in Toolik and Imnavait WS; Figure 3D,E) and additional differences at the permafrost boundary (50+ cm Toolik WS; 60+ cm Imnavait WS; 40+ cm Sagwon WS; Figure 3D–F). These significant taxonomic differences at the permafrost boundary are likely due to the limitations imposed on the microbiome from prolonged freezing (see also Kraft et al., 2015; Liang et al., 2019; Willerslev et al., 2004). Imnavait WS tundra was the only soil profile with several non-significant clusters of bacterial taxa by distinct depths, with only the 40–60 cm depths forming a significantly distinct cluster based on the relative abundance of shared bacterial taxa within these soil depths (95% similarity; Figure 4E).

TABLE 1 Relative abundance (mean ± SD) of dominant microbial taxa (order-level within phylum) separated between active layer (AL) and permafrost (PF) soil layers based on significant soil depth clusters obtained from hierarchical clustering analysis

		Toolik Lake				Imnavait Creek				Sagwon Hills			
		MAT Tundra		WS Tundra		MAT Tundra		WS Tundra		MAT Tundra		WS Tundra	
	Taxonomy	AL (0–40 cm)	PF (40–90 cm)	AL (0–50 cm)	PF (50–90 cm)	AL (0–40 cm)	PF (40–70 cm)	AL (0–60 cm)	PF (60–100 cm)	AL (0–30 cm)	PF (30–90 cm)	AL (0–40 cm)	PF (40–70 cm)
Active layer dominant taxa	Acidobacteriota												
	Acidobacteriales	7.8 ± 3.1^{a}	0.3 ± 0.2^{b}	1.1 ± 1.9	0.1 ± 0.1	10.4 ± 3.4^{a}	0.9 ± 1.1^{b}	8.0 ± 7.7	2.5 ± 1.1	0 ± 0	0 ± 0	2.1 ± 4.0	0 ± 0
	Solibacterales	1.6 ± 0.7^{a}	0.6 ± 0.2^{b}	0.6 ± 0.3^{a}	0 ± 0^{b}	1.7 ± 1.0	0.4 ± 0.4	2.2 ± 0.3^{a}	0.8 ± 0.6^{b}	0 ± 0	0.1 ± 0.1	0.4 ± 0.3	0 ± 0
	Vicinamibacterales	1.5 ± 1.4	0.8 ± 0.7	0.7 ± 0.4	0.7 ± 0.2	1.2 ± 0.7	0.7 ± 0.4	0.3 ± 0.2	0.4 ± 0.2	6.5 ± 2.4^{a}	2.4 ± 1.5^{b}	3.1 ± 1.3^{a}	1.1 ± 0.1^{b}
	Alphaproteobacteria												
	Rhizobiales	4.9 ± 0.8^{a}	1.2 ± 0.8^{b}	1.2 ± 2.0	0.1 ± 0.1	4.5 ± 2.6^{a}	0.6 ± 0.7^{b}	2.1 ± 2.8	0.6 ± 0.6	6.6 ± 2.6	3.8 ± 2.3	8.0 ± 2.2	8.5 ± 0.3
	Gammaproteobacteria												
	Burkholderiales	10.0 ± 4.6	8.8 ± 3.8	2.8 ± 4.3	1.1 ± 1.0	12.2 ± 9.6	11.4 ± 3.4	3.0 ± 3.6	1.3 ± 0.6	13.3 ± 2.6	15.6 ± 3	9.6 ± 4.8^{a}	1.5 ± 1.0^{b}
	Desulfobacterota												
	Geobacterales	0.5 ± 0.6	1.1 ± 0.5	2.2 ± 1.7	0.5 ± 0.6	1.0 ± 1.2	1.5 ± 0.3	3.0 ± 1.5^{a}	1.0 ± 0.5^{b}	2.6 ± 3.8	1.0 ± 0.7	0.1 ± 0.1^{a}	0.3 ± 0.1^{b}
	Syntrophales	0 ± 0^{a}	3.0 ± 0.5^{b}	7.2 ± 3.8	4.7 ± 0.8	1.4 ± 1.6	2.3 ± 0.7	7.6 ± 4.1	6.4 ± 3.6	0.1 ± 0.2^{a}	1.5 ± 0.5^{b}	0 ± 0^{a}	3.5 ± 0.4^{b}
	Gemmatimonadota												
	Gemmatimonadales	1.7 ± 1.9	0.5 ± 0.6	0.1 ± 0.1	0 ± 0	1.5 ± 1.2	0.1 ± 0.1	0.1 ± 0.1	0.1 ± 0.1	2.1 ± 0.9	0.9 ± 0.8	0.9 ± 0.7	0 ± 0
	Myxococcota												
	Myxococcales	0.9 ± 1.0	0 ± 0	0.3 ± 0.3	0 ± 0	0.7 ± 1.1	0.1 ± 0.1	0.3 ± 0.3	0 ± 0	0.1 ± 0.1	0.1 ± 0.1	0.5 ± 0.4	0.1 ± 0.1
	Planctomycetota												
	Tepidisphaerales	2.2 ± 1.1^{a}	0.9 ± 0.5^{b}	0.2 ± 0.1	0.2 ± 0.2	1.7 ± 2.0	1.4 ± 0.3	0.1 ± 0.1	0.3 ± 0.2	0.4 ± 0.1^{a}	0.1 ± 0.1^{b}	1.1 ± 1.6	0 ± 0
	Verrucomicrobiota												
	Chthoniobacterales	8.4 ± 4.1^{a}	0.3 ± 0.3^{b}	2.1 ± 2.2	0 ± 0	4.2 ± 5.0	0.6 ± 0.8	2.3 ± 0.9^{a}	0.7 ± 0.4^{b}	11.2 ± 3.7^{a}	1.4 ± 0.9^{b}	12.4 ± 12.4	0.3 ± 0.1
	Pedosphaerales	3.8 ± 1.1	2.0 ± 1.7	**7.6 ± 2.5^{a}**	**2.7 ± 2.5^{b}**	9.4 ± 6.2	3.6 ± 0.9	13.3 ± 6.8	13.0 ± 7.1	2.9 ± 0.9	2.3 ± 1.7	3.6 ± 1.6^{a}	0.8 ± 0.1^{b}
Permafrost dominant taxa	Actinobacteriota												
	Gaiellales	0.3 ± 0.2^{a}	11.4 ± 4.8^{b}	2.3 ± 0.9^{a}	17.4 ± 6.3^{b}	0.8 ± 0.8^{a}	3.4 ± 1.7^{b}	1.6 ± 1.0^{a}	4.4 ± 0.9^{b}	4.3 ± 1.7^{a}	8.2 ± 2.1^{b}	1.3 ± 0.8^{a}	7.5 ± 2.5^{b}
	Micrococcales	2.4 ± 2.5^{a}	8.3 ± 2.7^{b}	0.3 ± 0.1^{a}	3.7 ± 2.3^{b}	2.7 ± 3.0	3.3 ± 0.5	0.8 ± 0.8	3.5 ± 3.9	1.3 ± 1.7^{a}	7.6 ± 2.4^{b}	1.1 ± 1.3^{a}	4.3 ± 1.0^{b}
	RBG-16-55-12	0 ± 0^{a}	5.1 ± 3.1^{b}	2.0 ± 1.3^{a}	6.1 ± 1.5^{b}	0.1 ± 0.1^{a}	2.7 ± 0.9^{b}	0.4 ± 0.3	0.2 ± 0.1	0 ± 0	1.5 ± 1.8	0 ± 0^{a}	2.9 ± 0.2^{b}
	WCHB1-81	0 ± 0^{a}	0.8 ± 0.4^{b}	1.2 ± 0.8	1.3 ± 0.7	0 ± 0	0.8 ± 0.7	0.1 ± 0.1	0.3 ± 0.2	0 ± 0	2.5 ± 2.5	0 ± 0^{a}	10.4 ± 1.4^{b}
	Bacteroidota												
	Bacteroidales	0.1 ± 0.2^{a}	15.6 ± 5.2^{b}	10.7 ± 5.2^{a}	30.1 ± 4.7^{b}	4.3 ± 5.1^{a}	21.8 ± 1.1^{b}	8.8 ± 5.8	18.2 ± 8.9	0.5 ± 0.7^{a}	4.9 ± 1.1^{b}	0.1 ± 0.2^{a}	14.8 ± 2.2^{b}
	Sphingobacteriales	3.0 ± 2.3	0.8 ± 0.5	3.5 ± 1.8	1.9 ± 1.5	1.6 ± 1.1	0.8 ± 0.2	2.7 ± 1.3^{a}	7.1 ± 3.7^{b}	0.8 ± 0.6	1.2 ± 0.6	1.7 ± 1.5	0.2 ± 0.1
	Caldisericota												
	Caldisericales	0 ± 0	5.0 ± 6.6	2.0 ± 1.3	4.3 ± 2.4	0.1 ± 0.1^{a}	8.6 ± 2.9^{b}	0.5 ± 0.7^{a}	2.8 ± 0.7^{b}	0 ± 0	0.5 ± 0.6	0 ± 0^{a}	8.6 ± 3.3^{b}
	Firmicutes												
	Clostridiales	0.1 ± 0.1^{a}	7.5 ± 3.1^{b}	3.0 ± 2.8	3.5 ± 0.7	0.5 ± 0.6^{a}	7.3 ± 0.6^{b}	0.6 ± 0.5	3.8 ± 3.7	0 ± 0^{a}	1.0 ± 0.4^{b}	0 ± 0^{a}	2.8 ± 0.4^{b}

Note: Letters indicate significant differences between soil layers specifically within each tundra type at each site (ANOVA; $p < 0.05$).

The observed shift in composition between the active layer and permafrost microbiomes at all sites was largely due to variations in the abundance of Acidobacteriota, Actinobacteriota, and Bacteroidota (Figure 3), generally consistent with previous studies in arctic soils (Deng et al., 2015; Frank-Fahle et al., 2014; Kim et al., 2016; Müller et al., 2018; Singh et al., 2017; Tripathi et al., 2018, 2019; Varsadiya et al., 2021; Wilhelm et al., 2011). For example, we found that *Acidobacteriales*, *Solibacteriales*, and *Vicinamibacterales* (Acidobacteriota) abundance was greater in the active-layer microbiome compared to the permafrost microbiome, especially within MAT tundra, while *Gaiellales*, *Micrococcales*, RBG-16-55-12, and WCHB1-81 (Actinobacteriota), as well as *Bacteroidales* and *Sphingobacteriales* (Bacteroidota) abundance was greater in the permafrost microbiome of both tundra types (ANOVA; $p < 0.05$ where indicated; Table 1). However, we did find that dominant Acidobacteriota taxa in the active-layer soil depths differed between Toolik and Imnavait MAT tundra compared to Sagwon MAT tundra (Table 1). Specifically, Acidobacteriota within the active-layer microbiome of Toolik and Imnavait MAT tundra consisted of *Acidobacteriales* (7.8%–10.4%) and *Solibacteriales* (1.6%–1.7%), with less than 1.5% relative abundance of *Vicinamibacterales* (Table 1). The Sagwon MAT tundra active-layer microbiome contained no measurable abundance of *Acidobacteriales* or *Solibacteriales* but had ~6.5% of *Vicinamibacterales* (Table 1). The active-layer microbiome within Sagwon WS tundra was similar and contained ~3.1% relative abundance of *Vicinamibacterales* (Table 1). The similarly high relative abundance of *Vicinamibacterales* within Sagwon MAT and WS tundra may also account, in part, for their shared ordination patterns in our NMDS plot that clustered distinctly from either tundra type at Toolik and Imnavait (Figure 2C).

In addition to the Acidobacteriota, the relative abundance of Pseudomonadota (formerly Proteobacteria) such as *Rhizobiales* (Alphaproteobacteria) and *Burkholderiales* (Gammaproteobacteria), as well as *Geobacterales* (Desulfobacterota) and Verrucomicrobiota including *Chthoniobacterales* and *Pedosphaerales* were greater in the active-layer microbiome across the region (Table 1), consistent with studies conducted at numerous sites across the Arctic (reviewed by Malard & Pearce, 2018). The higher abundance of Pseudomonadota in the active layer could be related to their preference for higher concentrations of nutrients (Kim et al., 2016), especially given that the relative abundance of Alphaproteobacteria and Gammaproteobacteria taxa were shown to increase after fertilization compared with control plots at Toolik (Campbell et al., 2010; Koyama et al., 2014). Also, the greater abundance of bacterial taxa such as *Geobacterales* (Desulfobacterota) in the active-layer microbiome of WS tundra (Table 1) is likely because they thrive under saturated conditions common in the active layer of WS tundra (Emerson et al., 2015), as has been previously reported from the Toolik Lake region (Romanowicz et al., 2021). This suggests that the depth-dependent variations in the soil microbiome could be related to the different resource needs of each bacterial taxon.

In contrast, the permafrost microbiome was similar across sites due to an increase in the relative abundance of Actinobacteriota and Bacteroidota (Figure 3), as mentioned earlier. In addition, the relative abundance of Caldisericota and Firmicutes also increased in the permafrost microbiome (Figure 3) and clustered together consistently with the greater relative abundance of Actinobacteriota and Bacteroidota with depth (Figure 4). We note that Caldisericota (*Caldisericales*) in the permafrost microbiome (Figure 3; Table 1), also reported in numerous arctic studies (Monteux et al., 2018; Taş et al., 2018; Tripathi et al., 2018, 2019; Varsadiya et al., 2021), was recently proposed as *Candidatus* Cryosericota phylum (Martinez et al., 2019), although we retain the taxonomic annotation as Caldisericota throughout this study (see Appendix SI for full details). The high relative abundance of Actinobacteriota such as *Gaiellales* and *Micrococcales* in the permafrost microbiome (Table 1) is likely due to their ability to form dormant and spore-like structures (Wunderlin et al., 2014) that can survive radiation, starvation, and extreme desiccation (De Vos et al., 2009; Johnson et al., 2007). Likewise, *Bacteroidales* (Bacteroidota) and *Clostridiales* (Firmicutes) are known to form endospores under the stressful conditions associated with permafrost, and they persist at higher relative abundance than non-endospore forming taxa common in the active-layer microbiome that perish in the harsh conditions (Burkert et al., 2019). This loss of non-endospore forming taxa is compounded with time causing further convergence in the composition of the permafrost microbiome across the region as the permafrost ages (see Liang et al., 2019; Mackelprang et al., 2017).

Total cell counts by depth along each soil profile showed that the absolute abundance of bacterial cells was similar between the active layer and permafrost depths (~10^6 to 10^8 cells per gram of soil; Table S2), and only the relative abundance of bacterial taxa changed with depth (Figure 3). Likewise, bacterial cell viability assays (% live cells) showed similar numbers of live cells with increasing soil depth across all sampling locations (Table S2). Thus, the permafrost microbiome maintains a similar abundance of bacterial cells with similar proportions of live cells compared to the active-layer microbiome. However, the permafrost microbiome has developed into a relic composition consisting of only a subset of bacterial taxa originally present at the time of permafrost formation, such as has been shown previously (Burkert et al., 2019; Liang et al., 2019). Our results strongly suggest that the permafrost microbiome

has converged toward a shared subset of bacterial taxa capable of withstanding the harsh permafrost environment, and these taxa are no longer regulated by the same environmental factors affecting the overlying active-layer microbiomes across the region. The relative abundance of archaeal taxa was <3% at any given site or depth (Figure 3, Figure S2) but still differed statistically between tundra types (ANOVA; $p < 0.001$). Archaeal taxa consisted primarily of methanogenic Euryarchaeota such as *Methanobacteriales* and *Methanosarcinales*, consistent with similar observations across the tundra region (Deng et al., 2015; Hultman et al., 2015; Lipson et al., 2013; Romanowicz et al., 2021; Tripathi et al., 2018).

Methanobacteriales are hydrogenotrophic methanogens and *Methanosarcinales* are acetoclastic methanogens, both of which are commonly found in saturated organic peat soils (Conrad et al., 1987; Deng et al., 2015; Metje & Frenzel, 2007; Tveit et al., 2015). Here, these methanogenic archaeal taxa were found predominantly in the surface depths (0–50 cm) of WS tundra at Toolik and Imnavait, while archaeal taxa in general were negligible in MAT tundra across all sites (Figure S2). The greater relative abundance of both groups of methanogenic archaea in the WS tundra microbiome is likely due to relatively flat topography and the lack of soil drainage imposed by the permafrost boundary, both of which facilitate persistent saturation of the active layer and subsequent anoxia, providing substrates to carry out multiple fermentative pathways of methanogenesis.

Thaw frequency and the transition zone microbiome

Thaw depth measurements collected at three of our sampling sites annually in July and August since 1990 (Toolik MAT tundra) or 2003 (Imnavait MAT and WS tundra; see Appendix S1) show the annual and seasonal extent of thawed versus frozen soil (Table 2). The mean August thaw depth (±SD) over the survey duration was 40.5 cm (±5.3 cm) for Toolik MAT tundra, 43.9 cm (±6.2 cm) for Imnavait MAT tundra, and 56.3 cm (±5.7 cm) for Imnavait WS tundra. Thaw depth increased at a mean rate of 0.34 cm yr^{-1} for Toolik MAT tundra, 0.85 cm yr^{-1} for Imnavait MAT tundra, and 0.84 cm yr^{-1} for Imnavait WS tundra. The thaw survey data over time show the frequency of summer thaw to any depth, and we converted thaw depth measurements (cm) into thaw probabilities (% of thaw occurrence in any 1 year) for each 10-cm increment of the soil profile over the survey duration (Table 2). Depths that thawed intermittently in August (i.e. not every year) were considered to be in the 'transition zone' between high probability of thaw in a year for the active layer and low probability of thaw in a year for the permafrost. Within MAT tundra, thaw probabilities for July and August in the soil profiles were similar between Toolik and Imnavait, with the active layer extending from 0 to 40 cm, the transition zone from 40 to 60 cm, and permafrost from 60+ cm depth (Table 2). For Imnavait WS tundra, we found the active layer extended from 0 to 50 cm, the transition zone from 50 to 70 cm, and permafrost from 70+ cm depth (Table 2). None of the transition-zone depths at any sampling location experienced thaw at the July sampling point for the entire duration of thaw surveys (July thaw probability = 0%; Table 2). By comparing soil depths within each soil layer as determined from thaw surveys, with results from the hierarchical clustering analysis of microbial taxa (Figure 4A,B,E), we demonstrate statistically that microbial composition in the transition-zone depths always clusters with the composition of the permafrost depths for the three sampling locations having thaw survey data. This indicates that the microbiome composition of the transition zone was statistically indistinguishable from the composition in the permafrost.

Results from the transition-zone microbiome confirm our prediction that the permafrost microbiome has not been substantially altered in composition when exposed to intermittent freeze–thaw cycles. This differs from previous laboratory-based experiments of the permafrost microbiome that show rapid shifts in the composition and associated biogeochemical functions of microbial taxa within a few days of simulated thaw (Coolen & Orsi, 2015; Hultman et al., 2015; Mackelprang et al., 2011; Waldrop et al., 2010). Our results are more consistent with previous field-based warming experiments that show little or no change in permafrost microbiome composition following moderate heating of the active layer that mimics its natural extension into the permafrost (Biasi et al., 2008; Lamb et al., 2011; Rinnan et al., 2007). As such, this study demonstrates that in natural settings, it takes more than just intermittent thaw, for example ~0.1–0.8 probability that the soil will thaw in any single year (Table 2), to induce compositional change in the transition-zone microbiome.

Our transition-zone microbiome results also contrast with a previous soil profile survey from high Arctic heath at Svalbard, Norway (Müller et al., 2018), where microbial taxa in the thaw transition zone differed in their relative abundance by >60% from the permafrost microbiome. This difference could be because their transition zone is narrower than ours, or they had finer resolution of the soil profile sampling at 3-cm intervals rather than the 10-cm interval we used. Homogenization of microbial taxa within a 10-cm soil increment that spans the depths of the transition zone and permafrost soil layers may have hidden subtle changes in taxonomic abundance between these soil layers. However, our thaw surveys showed that depths with intermittent

TABLE 2 Average thaw probability (%) within each 10-cm increment along the soil profile for moist acidic tussock (MAT) tundra at Toolik and Imnavait and wet sedge (WS) tundra at Imnavait measured annually on 2 July and 11 August (±1 day) since 1990 (Toolik) or 2003 (Imnavait)

	Toolik Lake			Imnavait Creek					
	Moist acidic tussock tundra			Moist acidic tussock tundra			Wet sedge tundra		
Soil profile depth (cm)	July thaw probability (%) 1990–2018	August thaw probability (%) 1990–2018	Annual thaw duration (days) 2018	July thaw probability (%) 2003–2018	August thaw probability (%) 2003–2018	Annual thaw duration (days) 2018	July thaw probability (%) 2003–2018	August thaw probability (%) 2003–2018	Annual thaw duration (days) 2018
0–10	100	100	80	100	100	62	100	100	62
10–20	100	100	80	100	100	62	100	100	62
20–30	45.2	100	69	76.5	100	53	100	100	53
30–40	3.2	96.8	46	5.9	100	35	52.9	100	44
40–50	0	61.3	34	0	64.7	27	5.9	100	35
50–60	0	3.2	0	0	11.8	0	0	82.4	27
60–70	0	0	0	0	0	0	0	35.3	18
70–80	0	0	0	0	0	0	0	0	0
80–90	0	0	0	0	0	0	0	0	0
90–100	0	0	0	0	0	0	0	0	0

Note: Thaw duration (minimum number of thaw days per year) within each 10-cm increment along the soil profile for all three sites was determined from seven measurements taken from 2 June to 20 August 2018 (Toolik) or 21 June to 21 August 2018 (Imnavait). Highlighted rows represent the transition zone (0% <August thaw probability <100%; light grey) and permafrost (0% August thaw probability; dark grey) soil layers.

thaw ranged from a minimum of 15 cm (Imnavait WS tundra) up to 23 cm (Toolik MAT tundra) through the soil profiles; these depths exceed any single 10-cm soil increment, and thus potential homogenization of the transition-zone depths with the permafrost depths should be minimized. These results are the first to show that composition of the transition-zone microbiome has not significantly shifted from the permafrost microbiome even though these soil depths have experienced intermittent thaw for on average 61% of the past 28 years at Toolik or 65%–82% of the past 15 years at Imnavait (Table 2).

Thaw duration

In addition to the frequency of thaw, we determined the thaw duration (i.e. minimum number of thaw days in a summer) that each 10-cm increment along the soil profile experienced in 2018 (Table 2); the year 2018 corresponds to the field season when soil profiles were sampled for their microbiome composition. These are 'minimum' estimates because a depth may have thawed in between successive thaw survey dates or after the final survey (see Appendix S1). The transition-zone depths had less than half the number of thaw days than the average thaw days of the active layer. Specifically, the Toolik MAT tundra transition zone (40–60 cm) on average thawed only a quarter of the time (24.7%) that the active layer (0–40 cm) thawed (Table 2). In Imnavait MAT tundra the transition zone (40–60 cm) had only 25.5% of mean active layer (0–40 cm) thaw days, and Imnavait WS tundra transition zone (50–70 cm) had 43.9% of mean active layer (0–50 cm) thaw days (Table 2). This decline of thaw duration in the transition zone depths compared to the active-layer depths, as well as the complete lack of thaw in the transition zone depths in July over all survey years, may account for the similar composition of the transition zone microbiome with the permafrost microbiome in hierarchical clustering analysis (Figure 4).

Spearman's non-parametric rank correlations between thaw duration and the relative abundance of microbial taxa by depth along the soil profiles showed consistent, significant patterns between the three sampling locations associated with thaw survey data. In MAT tundra, Acidobacteriota, Alphaproteobacteria, and Verrucomicrobiota were significantly positively correlated with thaw duration at Toolik (Figure 5A) and Imnavait (Figure 5B), with Myxococcota and Planctomycetota also significantly positively correlated with thaw duration at Toolik (Figure 5A). This indicates that their relative abundance was greatest in soil depths experiencing the greatest duration of thaw (i.e. active-layer depths). In WS tundra at Imnavait, Acidobacteriota, Myxococcota, and Alphaproteobacteria were also significantly

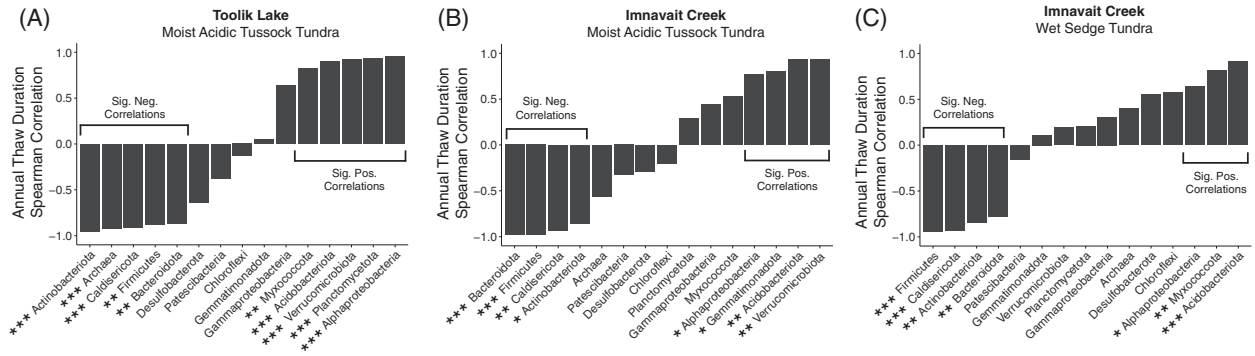

FIGURE 5 Spearman non-parametric rank correlation plots between thaw duration and microbial taxa along the soil profile of moist acidic tussock (MAT) tundra at Toolik (A) and Imnavait (B) and wet sedge (WS) tundra at Imnavait (C). Correlations are arranged from Spearman's rho values of −1 to 1 among microbial taxa within each plot to emphasize those microbial taxa significantly negatively or positively correlated with thaw duration, respectively. Asterisks indicate the significance of the negative or positive correlation between thaw duration and mean relative abundance of each microbial taxon along the soil profile (Spearman rho; ***$p < 0.001$, **$p < 0.01$, *$p < 0.05$).

positively correlated with thaw duration, but Verrucomicrobiota and Planctomycetota were not (Figure 5C). These correlations, or lack thereof, distinguishes the dominant WS tundra microbial taxa from the dominant MAT tundra microbial taxa in the active layer by hierarchical clustering analysis (Figure 4A,B,E). In contrast, Actinobacteriota, Bacteroidota, Caldisericota, and Firmicutes were significantly negatively correlated with thaw duration at all three sampling locations (Figure 5A–C). This indicates that their relative abundance was greatest in soil depths experiencing the shortest duration of thaw each year (i.e. permafrost depths).

The significant positive and negative correlations between thaw duration and the relative abundance of microbial taxa at each soil depth are consistent with the significant clusters of microbial taxa in the active layer and the permafrost depths derived from hierarchical clustering analysis, respectively (Figure 4A,B,E). These correlation results are also consistent with significant depth-dependent differences in the relative abundance of dominant bacterial taxa between the active layer and permafrost depths (Table 1). For example, the significant positive correlation between thaw duration and the abundance of Alphaproteobacteria at all three sites (Figure 5A–C) was consistent with a greater abundance of *Rhizobiales* (Alphaproteobacteria) in the active layer depths of those same sites (ANOVA; $p < 0.05$ for MAT tundra sites; Table 1). This suggests that the greater abundance of Alphaproteobacteria, specifically the *Rhizobiales*, in the active layer depths is in part a direct result of the greater duration of annual thaw at these corresponding depths along the soil profile. Likewise, the significant positive correlation between thaw duration and the abundance of Acidobacteriota (Figure 5A–C) likely accounts for the significantly greater abundance of *Acidobacteriales* and *Solibacterales* in the active layer depths of all three sites associated with thaw duration measurements (Table 1).

In a similar way, but with the opposite effect, the significant negative correlations between thaw duration and the abundance of Actinobacteriota, Bacteroidota, Caldisericota, and Firmicutes at all three sites (Figure 5A–C) is most likely due to the low or non-existent thaw duration in the transition zone and permafrost soil depths (Table 2). Prolonged freezing in permafrost soils significantly decreases dispersal and imposes substantial thermodynamic constraints that influence the composition of the permafrost microbiome (Bottos et al., 2018). As such, the permafrost microbiome converges toward a relic composition dominated by dormant and spore-forming taxa such as *Gaiellales* and *Micrococcales* (Actinobacteriota), *Bacteroidales* (Bacteroidota), *Caldisericales* (Caldisericota), and *Clostridiales* (Firmicutes) (see Table 1) that can survive radiation, starvation, and extreme desiccation (De Vos et al., 2009; Johnson et al., 2007). The loss of non-endospore forming taxa is compounded with time causing further convergence in the composition of the permafrost microbiome across the region as the permafrost ages (see Liang et al., 2019; Mackelprang et al., 2017). Thus, the lack of substantial thaw duration and the assumed effects associated with prolonged freezing in the transition zone and permafrost soil depths accounts for the consistent negative correlations between thaw duration and the relative abundance of each of these dominant phyla (Actinobacteriota, Bacteroidota, Caldisericota, Firmicutes; Figure 5A–C) at sites associated with thaw duration measurements.

Previous studies that focused on changes in soil physicochemical properties such as pH, conductivity, water content, and organic C to explain depth-dependent variations in the soil microbiome concluded that the majority of the variation remained unexplained by these environmental factors (reviewed by Malard & Pearce, 2018). We also found weak correlations between soil physicochemical properties and microbial

TABLE 3 Spearman non-parametric rank correlations between soil physicochemical properties and microbial taxa at the three sampling locations associated with multi-decadal thaw measurements

	Soil pH			Soil conductivity			Soil water content			Organic carbon content		
Taxonomy	**Toolik MAT**	**Imnavait MAT**	**Imnavait WS**	**Toolik MAT**	**Imnavait MAT**	**Imnavait WS**	**Toolik MAT**	**Imnavait MAT**	**Imnavait WS**	**Toolik MAT**	**Imnavait MAT**	**Imnavait WS**
Acidobacteriota	−0.67*	−0.92**	0.30	0.05	−0.04	−0.15	−0.18	0.79*	0.16	−0.12	0.82*	0.78*
Actinobacteriota	0.79*	0.74	0.09	−0.02	0.32	0.43	−0.23	−0.71	0.14	−0.17	−0.75	−0.56
Bacteroidota	0.72*	0.96***	−0.16	0.12	0.07	0.22	0.27	−0.82*	−0.03	0.17	−0.89*	−0.49
Caldisericota	0.75*	0.95**	−0.1	0.24	−0.05	0.25	−0.02	−0.81*	0.08	0.07	−0.85*	−0.64
Chloroflexi	0.18	0.27	0.13	−0.97***	−0.36	−0.60	−0.63	−0.11	−0.35	−0.82*	−0.14	0.39
Desulfobacterota	0.96***	0.34	−0.22	−0.30	−0.39	−0.76*	−0.25	−0.36	−0.54	−0.35	−0.32	0.15
Firmicutes	0.69*	0.99***	0.02	0.13	−0.11	0.35	0.03	−0.86*	0.07	0.07	−0.93**	−0.52
Gemmatimonadota	0.23	−0.75*	−0.12	−0.75*	−0.14	0.33	−0.83**	0.68	−0.18	−0.90**	0.75	0.04
Myxococcota	−0.67*	−0.63	0.44	0.17	0.36	−0.04	0.13	0.39	0.20	0.13	0.43	0.79**
Patescibacteria	0.51	0.36	−0.88**	−0.58	−0.29	−0.3	−0.68	−0.43	−0.59	−0.73*	−0.36	−0.53
Planctomycetota	−0.73*	−0.34	−0.58	0	0.39	0.25	0.2	0.36	0.03	0.12	0.32	0.03
Verrucomicrobiota	−0.68	−0.94**	−0.60	0.08	0.07	−0.76*	−0.05	0.79*	−0.72*	−0.02	0.86*	−0.38
Alphaproteobacteria	−0.71*	−0.87*	0.49	0.17	0.46	−0.05	0.08	0.75	0.24	0.10	0.79*	0.59
Gammaproteobacteria	−0.51	−0.41	0.13	−0.23	−0.14	0.30	0.00	0.32	0.30	−0.05	0.43	0.31
Archaea	0.81**	0.50	−0.22	−0.03	0.00	−0.50	−0.10	−0.50	−0.26	−0.13	−0.54	0.22

Note: When the correlation coefficient (rho) equals 1, it is considered a completely positive correlation; when it equals −1, it is considered a completely negative correlation. Asterisks indicate the significance of the correlation, positive or negative (spearman; ***$p < 0.001$; **$p < 0.01$; *$p < 0.05$).

taxa (Table 3). For the three sampling locations associated with multi-decadal thaw surveys, we found a significant correlation between a physicochemical property and a certain taxon at only one or two locations instead of significant correlations at all three locations. For example, differences in soil pH by depth were significantly negatively correlated with active-layer dominant Acidobacteriota and Alphaproteobacteria at both MAT tundra sites (Toolik and Imnavait) but not significantly correlated (positively or negatively) by soil depth at Imnavait WS tundra (Table 3). Likewise, differences in soil pH by depth were significantly positively correlated with the permafrost-dominant taxa Bacteroidota, Caldisericota, and Firmicutes at both MAT tundra sites, but not at Imnavait WS tundra (Table 3). Previous studies showed that the relative abundance of Acidobacteriota had a strong positive correlation with soil pH and these taxa dominated the more acidic surface depths of the active layer before declining in abundance with depth toward the permafrost (Kim et al., 2016; Neufeld & Mohn, 2005; Wallenstein et al., 2007). In our results, we found a similar correlation between soil pH and Acidobacteriota with soil depth at all our MAT tundra sites.

There were also significant correlations with other environmental factors and microbial taxa by soil depth at some sites (Table 3); however, there were no general patterns of correlation across all sites. For example, those taxa that were significantly correlated with soil conductivity, water content, or organic C content with soil depth in Toolik MAT tundra were not the same taxa that were significantly correlated by soil depth in Imnavait MAT tundra (Table 3). Inconsistent patterns occur between many taxa and the physicochemical properties measured at each sampling location (Table 3), making it difficult to draw conclusions about how these environmental factors regulate soil microbial abundance in MAT or WS tundra across the region. This analysis indicates that the measured soil physicochemical properties explain a relatively small amount of the among and within site variance in microbiome composition.

In contrast to soil physicochemical properties, the measured thaw frequency and especially thaw duration by depth (Figure 5) showed consistent correlations with the composition of the active layer and permafrost microbiomes. The transition zone experienced less than half the number of thaw days than the average for the active layer (Table 2). This considerable difference in thaw duration between the active layer and transition zone may explain why the transition zone microbiome was statistically indistinguishable from the permafrost microbiome (Figure 4). However, as the thaw duration in the transition zone increases with future warming, we suggest that the abundance of active-layer dominant taxa will increase including Alphaproteobacteria in MAT tundra (*Rhizobiales*), Desulfobacterota in WS tundra (*Geobacterales*), as well as Acidobacteriota (*Acidobacteriales* and *Solibacteriales*), Myxococcota (*Myxococcales*), Planctomycetota (*Tepidisphaerales*) and Verrucomicrobiota (*Chthoniobacterales* and *Pedosphaerales*) in both tundra types (Table 1). We also predict that an increase in thaw duration will likely decrease the relative abundance of Actinobacteriota (*Gaiellales* and *Micrococcales*), Bacteroidota (*Bacteroidales*), Caldisericota (*Caldisericales*), and Firmicutes (*Clostridiales*) in the transition zone of both MAT and WS tundra (Table 1). These predicted increases and decreases in taxa will shift the transition-zone microbiome away from the current, relic permafrost microbiome and towards the active-layer composition.

CONCLUSION

Results from our study are the first to show that thaw duration is a strong environmental factor that operates over time and space to regulate the microbial composition of the active layer, transition zone, and permafrost in soils of arctic tundra. The duration of thaw that soils experience each summer correlates better than does soil physicochemistry with the dominant microbial taxa among regional sites, tundra types, and soil depth. Furthermore, long-term thaw surveys indicate that while thaw depth is increasing over time, the transition-zone microbiome is still very similar to the permafrost microbiome. This suggests that thaw frequency and duration in the transition zone are still too low to shift the transition-zone microbiome composition away from that in the permafrost and towards that in the active layer. As climate warming increases and thaw frequency and especially thaw duration increases at depth, we predict that for any tundra soil the microbiome composition (and thus function) will shift from the relic permafrost taxa towards current active-layer taxa. These shifts should follow the current thaw duration and microbial composition at each depth (e.g. Table 2, Figure 3). Monitoring thaw duration and microbiome composition at depth may help predict the microbial response to future permafrost thaw.

ACKNOWLEDGEMENTS

The authors thank B. Crump, R. Cory, N. Jelinski, J. Dobkowski, C. Cook, L. Treibergs, J. Albrigtsen, J. Jastrow, R. Matamala, T. Vugteveen, J. Lederhouse, and colleagues of the NSF Arctic LTER and Toolik Lake Field Station for assistance. Additional thanks to G. Romanowicz and G. Sobocinski for support with fluorescence microscopy. The authors also thank B. Crump and T. Schmidt, as well as three anonymous reviewers, for providing helpful comments on an earlier version of this manuscript. The authors acknowledge the University of Michigan Microbiome Core and Advanced Research Computing Technology Services.

Support for this work came from NSF grants DEB-1637459, DEB-1754835, and OPP-1936769 and DOE grant DE-AC02-06CH11357.

CONFLICT OF INTEREST

The author declares that there is no conflict of interest that could be perceived as prejudicing the impartiality of the research reported.

DATA AVAILABILITY STATEMENT

All raw forward and reverse sequencing reads are deposited in the NCBI Sequence Read Archive (SRA) and are publicly available through BioProject accession PRJNA794857. Input files and rendered code for replicating all statistical analyses using the R environment (v 4.2.1) are publicly available through the following link: https://github.com/kromanowicz/2022-Annual-Thaw-Microbes.

REFERENCES

Apprill, A., McNally, S., Parsons, R. & Weber, L. (2015) Minor revision to V4 region SSU rRNA 806R gene primer greatly increases detection of SAR11 bacterioplankton. *Aquatic Microbial Ecology*, 75(2), 129–137.

Barichivich, J., Briffa, K.R., Osborn, T.J., Melvin, T.M. & Caesar, J. (2012) Thermal growing season and timing of biospheric carbon uptake across the Northern Hemisphere. *Global Biogeochemical Cycles*, 26, GB4015.

Biasi, C., Meyer, H., Rusalimova, O., Hämmerle, R., Kaiser, C., Baranyi, C. et al. (2008) Initial effects of experimental warming on carbon exchange rates, plant growth and microbial dynamics of a lichen-rich dwarf shrub tundra in Siberia. *Plant and Soil*, 307, 191–205.

Bisanz, J.E. (2018) qiime2R: importing QIIME2 artifacts and associated data into R sessions. Version 0.99, 13.

Bolyen, E., Rideout, J.R., Dillon, M.R., Bokulich, N.A., Abnet, C.C., al-Ghalith, G.A. et al. (2019) Reproducible, interactive, scalable and extensible microbiome data science using QIIME 2. *Nature Biotechnology*, 37(8), 852–857.

Bottos, E.M., Kennedy, D.W., Romero, E.B., Fansler, S.J., Brown, J. M., Bramer, L.M. et al. (2018) Dispersal limitation and thermodynamic constraints govern spatial structure of permafrost microbial communities. *FEMS Microbiology Ecology*, 94, fiy110.

Burkert, A., Douglas, T.A., Waldrop, M.P. & Mackelprang, R. (2019) Changes in the active, dead, and dormant microbial community structure across a Pleistocene permafrost chronosequence. *Applied and Environmental Microbiology*, 85(7), e02646–e02618.

Callahan, B.J., McMurdie, P.J., Rosen, M.J., Han, A.W., Johnson, A. J.A. & Holmes, S.P. (2016) DADA2: high-resolution sample inference from Illumina amplicon data. *Nature Methods*, 13(7), 581–583.

Campbell, B.J., Polson, S.W., Hanson, T.E., Mack, M.C. & Schuur, E. A. (2010) The effect of nutrient deposition on bacterial communities in Arctic tundra soil. *Environmental Microbiology*, 12, 1842–1854.

Castro, H.F., Classen, A.T., Austin, E.E., Norby, R.J. & Schadt, C.W. (2010) Soil microbial community responses to multiple experimental climate change drivers. *Applied and Environmental Microbiology*, 76, 999–1007.

Chen, Y., Liu, F., Kang, L., Zhang, D., Kou, D., Mao, C. et al. (2021) Large-scale evidence for microbial response and associated carbon release after permafrost thaw. *Global Change Biology*, 27(14), 3218–3229.

Chiarello, M., McCauley, M., Villéger, S. & Jackson, C.R. (2022). Ranking the biases: The choice of OTUs vs. ASVs in 16S rRNA amplicon data analysis has stronger effects on diversity measures than rarefaction and OTU identity threshold. *PLoS One*, 17(2), p.e0264443.

Chu, H., Fierer, N., Lauber, C.L., Caporaso, J.G., Knight, R. & Grogan, P. (2010) Soil bacterial diversity in the Arctic is not fundamentally different from that found in other biomes. *Environmental Microbiology*, 12, 2998–3006.

Chu, H., Neufeld, J.D., Walker, K. & Grogan, P. (2011) The influence of vegetation type on the dominant soil bacteria, archaea, and fungi in a low Arctic tundra landscape. *Soil Science Society of America Journal*, 75(5), 1756–1765.

Conrad, R., Schutz, H. & Babbel, M. (1987) Temperature limitation on hydrogen turnover and methanogenesis in anoxic paddy soil. *FEMS Microbiology Ecology*, 3, 281–289.

Coolen, M.J. & Orsi, W.D. (2015) The transcriptional response of microbial communities in thawing Alaskan permafrost soils. *Frontiers in Microbiology*, 6, 197.

De Vos, P., Garrity, G.M., Jones, D., Krieg, N.R., Ludwig, W., Rainey, F.A. et al. (2009) Bergey's manual of systematic bacteriology. In: *The Firmicutes*, Vol. 3, 2nd edition. Dordrecht, Netherlands: Springer.

Deng, J., Gu, Y., Zhang, J., Xue, K., Qin, Y., Yuan, M. et al. (2015) Shifts of tundra bacterial and archaeal communities along a permafrost thaw gradient in Alaska. *Molecular Ecology*, 24, 222–234.

Emerson, D., Scott, J.J., Benes, J. & Bowden, W.B. (2015) Microbial iron oxidation in the Arctic tundra and its implications for biogeochemical cycling. *Applied and Environmental Microbiology*, 81, 8066–8075.

Euskirchen, E.S., McGuire, A.D., Kicklighter, D.W., Zhuang, Q., Clein, J.S., Dargaville, R.J. et al. (2006) Importance of recent shifts in soil thermal dynamics on growing season length, productivity, and carbon sequestration in terrestrial high-latitude ecosystems. *Global Change Biology*, 12, 731–750.

Frank-Fahle, B.A., Yergeau, E., Greer, C.W., Lantuit, H. & Wagner, D. (2014) Microbial functional potential and community composition in permafrost-affected soils of the NW Canadian Arctic. *PLoS One*, 9, e84761.

Ganzert, L., Bajerski, F. & Wagner, D. (2014) Bacterial community composition and diversity of five different permafrost-affected soils of Northeast Greenland. *FEMS Microbiology Ecology*, 89, 426–441.

Gittel, A., Bárta, J., Kohoutová, I., Mikutta, R., Owens, S., Gilbert, J. et al. (2014) Distinct microbial communities associated with buried soils in the Siberian tundra. *The ISME Journal*, 8, 841–853.

Hinzman, L.D., Bettez, N.D., Bolton, W.R., Chapin, F.S., Dyurgerov, M.B., Fastie, C.L. et al. (2005) Evidence and implications of recent climate change in northern Alaska and other Arctic regions. *Climatic Change*, 72, 251–298.

Hugelius, G., Strauss, J., Zubrzycki, S., Harden, J.W., Schuur, E.A. G., Ping, C.L. et al. (2014) Estimated stocks of circumpolar permafrost carbon with quantified uncertainty ranges and identified data gaps. *Biogeosciences*, 11, 6573–6593.

Hultman, J., Waldrop, M.P., Mackelprang, R., David, M.M., McFarland, J., Blazewicz, S.J. et al. (2015) Multi-omics of permafrost, active layer and thermokarst bog soil microbiomes. *Nature*, 521(7551), 208–212.

Jansson, J.K. & Tas, N. (2014) The microbial ecology of permafrost. *Nature Reviews Microbiology*, 12, 414–425.

Johnson, S.S., Hebsgaard, M.B., Christensen, T.R., Mastepanov, M., Nielsen, R., Munch, K. et al. (2007) Ancient bacteria show evidence of DNA repair. *Proceedings of the National Academy of Sciences of the United States of America*, 104, 14401–14405.

Jorgenson, M.T., Shur, Y.L. & Pullman, E.R. (2006) Abrupt increase in permafrost degradation in Arctic Alaska. *Geophysical Research Letters*, 33(2), L02503.

Judd, K.E., Crump, B.C. & Kling, G.W. (2006) Environmental drivers control eco- system function in bacteria through changes in community composition. *Ecology*, 87, 2068–2079.

Judd, K.E. & Kling, G.W. (2002) Production and export of dissolved C in arctic tundra mesocosms: the roles of vegetation and water flow. *Biogeochemistry*, 60, 213–234.

Kim, H.M., Lee, M.J., Jung, J.Y., Hwang, C.Y., Kim, M., Ro, H.M. et al. (2016) Vertical distribution of bacterial community is associated with the degree of soil organic matter decomposition in the active layer of moist acidic tundra. *Journal of Microbiology*, 54(11), 713–723.

Kolde, R. & Kolde, M.R. (2015) Pheatmap: pretty Heatmaps.

Koyama, A., Wallenstein, M.D., Simpson, R.T. & Moore, J.C. (2014) Soil bacterial community composition altered by increased nutrient availability in Arctic tundra soils. *Frontiers in Microbiology*, 5, 516.

Kraft, N.J., Adler, P.B., Godoy, O., James, E.C., Fuller, S. & Levine, J.M. (2015) Community assembly, coexistence and the environmental filtering metaphor. *Functional Ecology*, 29, 592–599.

Lamb, E.G., Han, S., Lanoil, B.D., Henry, G.H.R., Brummell, M.E., Banerjee, S. et al. (2011) A high arctic soil ecosystem resists long-term environmental manipulations. *Global Change Biology*, 17(10), 3187–3194.

Liang, R., Lau, M., Vishnivetskaya, T., Lloyd, K.G., Wang, W., Wiggins, J. et al. (2019) Predominance of anaerobic, spore-forming bacteria in metabolically active microbial communities from ancient Siberian permafrost. *Applied and Environmental Microbiology*, 85, e00560–e00519.

Lipson, D.A., Haggerty, J.M., Srinivas, A., Raab, T.K., Sathe, S. & Dinsdale, E.A. (2013) Metagenomic insights into anaerobic metabolism along an arctic peat soil profile. *PLoS One*, 8, e64659.

Liu, C., Cui, Y., Li, X. & Yao, M. (2021) microeco: an R package for data mining in microbial community ecology. *FEMS Microbiology Ecology*, 97(2), fiaa255.

Mackelprang, R., Burkert, A., Haw, M., Mahendrarajah, T., Conaway, C.H., Douglas, T.A. et al. (2017) Microbial survival strategies in ancient permafrost: insights from metagenomics. *The ISME Journal*, 11, 2305–2318.

Mackelprang, R., Waldrop, M.P., DeAngelis, K.M., David, M.M., Chavarria, K.L., Blazewicz, S.J. et al. (2011) Metagenomic analysis of a permafrost microbial community reveals a rapid response to thaw. *Nature*, 480(7377), 368–371.

Malard, L.A., Anwar, M.Z., Jacobsen, C.S. & Pearce, D.A. (2019) Biogeographical patterns in soil bacterial communities across the Arctic region. *FEMS Microbiology Ecology*, 95(9), fiz128.

Malard, L.A. & Pearce, D.A. (2018) Microbial diversity and biogeography in Arctic soils. *Environmental Microbiology Reports*, 10(6), 611–625.

Martinez, M.A., Woodcroft, B.J., Ignacio Espinoza, J.C., Zayed, A.A., Singleton, C.M., Boyd, J.A. et al. (2019) Discovery and ecogenomic context of a global Caldiserica-related phylum active in thawing permafrost, Candidatus Cryosericota phylum nov., Ca. Cryosericia class nov., Ca. Cryosericales ord. nov., Ca. Cryosericaceae fam. nov., comprising the four species Cryosericum septentrionale gen. nov. sp. nov., Ca. C. hinesii sp. nov., Ca. C. odellii sp. nov., Ca. C. terrychapinii sp. nov. *Systematic and Applied Microbiology*, 42, 54–66.

Metje, M. & Frenzel, P. (2007) Methanogenesis and methanogenic pathways in a peat from subarctic permafrost. *Environmental Microbiology*, 9, 954–964.

Monteux, S., Weedon, J.T., Blume-Werry, G., Gavazov, K., Jassey, V.E.J., Johansson, M. et al. (2018) Long-term in situ permafrost thaw effects on bacterial communities and potential aerobic respiration. *The ISME Journal*, 12, 2129–2141.

Müller, O., Bang-Andreasen, T., White, R.A., Elberling, B., Taş, N., Kneafsey, T. et al. (2018) Disentangling the complexity of permafrost soil by using high resolution profiling of microbial community composition, key functions and respiration rates. *Environmental Microbiology*, 20, 4328–4342.

Neufeld, J.D. & Mohn, W.W. (2005) Unexpectedly high bacterial diversity in Arctic tundra relative to boreal forest soils, revealed by serial analysis of ribosomal sequence tags. *Applied and Environmental Microbiology*, 71, 5710–5718.

Nielsen, U.N. & Ball, B.A. (2015) Impacts of altered precipitation regimes on soil communities and biogeochemistry in arid and semi-arid ecosystems. *Global Change Biology*, 21, 1407–1421.

Oksanen, J., Blanchet, F.G., Kindt, R., Legendre, P., Minchin, P.R., O'Hara, R.B., et al. (2019) Vegan: community ecology package. R Package, Version 2.5–5.

Osterkamp, T.E. & Romanovsky, V.E. (1999) Evidence for warming and thawing of discontinuous permafrost in Alaska. *Permafrost and Periglacial Processes*, 10(1), 17–37.

Parada, A.E., Needham, D.M. & Fuhrman, J.A. (2016) Every base matters: assessing small subunit rRNA primers for marine microbiomes with mock communities, time series and global field samples. *Environmental Microbiology*, 18(5), 1403–1414.

Pedregosa, F., Varoquaux, G., Gramfort, A., Michel, V., Thirion, B., Grisel, O. et al. (2011) Scikit-learn: machine learning in Python. *Journal of Machine Learning Research*, 12, 2825–2830.

Quast, C., Pruesse, E., Yilmaz, P., Gerken, J., Schweer, T., Yarza, P. et al. (2012) The SILVA ribosomal RNA gene database project: improved data processing and web-based tools. *Nucleic Acids Research*, 41(D1), D590–D596.

Ricketts, M.P., Matamala, R., Jastrow, J.D., Antonopoulos, D.A., Koval, J., Ping, C.L. et al. (2020) The effects of warming and soil chemistry on bacterial community structure in Arctic tundra soils. *Soil Biology and Biochemistry*, 148, 107882.

Rinnan, R., Michelsen, A., Bååth, E. & Jonasson, S. (2007) Fifteen years of climate change manipulations alter soil microbial communities in a subarctic heath ecosystem. *Global Change Biology*, 13(1), 28–39.

Romanowicz, K.J., Crump, B.C. & Kling, G.W. (2021) Rainfall alters permafrost soil redox conditions, but meta-omics show divergent microbial community responses by tundra type in the Arctic. *Soil Systems*, 5, 1–17.

Saidi-Mehrabad, A., Neuberger, P., Hajihosseini, M., Froese, D. & Lanoil, B.D. (2020) Permafrost microbial community structure changes across the Pleistocene-Holocene boundary. *Frontiers in Environmental Science*, 8(133), 1–11.

Schostag, M., Priemé, A., Jacquiod, S., Russel, J., Ekelund, F. & Jacobsen, C.S. (2019) Bacterial and protozoan dynamics upon thawing and freezing of an active layer permafrost soil. *The ISME Journal*, 13(5), 1345–1359.

Schuur, E.A.G., Bockheim, J., Canadell, J.G., Euskirchen, E., Field, C.B., Goryachkin, S.V. et al. (2008) Vulnerability of permafrost carbon to climate change: implications for the global carbon cycle. *Bioscience*, 58(8), 701–714.

Serreze, M.C., Walsh, J.E., Chapin, F.S., Osterkamp, T., Dyurgerov, M., Romanovsky, V. et al. (2000) Observational evidence of recent change in the northern high-latitude environment. *Climatic Change*, 46, 159–207.

Siciliano, S.D., Palmer, A.S., Winsley, T., Lamb, E., Bissett, A., Brown, M.V. et al. (2014) Soil fertility is associated with fungal and bacterial richness, whereas pH is associated with community composition in polar soil microbial communities. *Soil Biology and Biochemistry*, 78, 10–20.

Singh, P., Singh, S.M., Singh, R.N., Naik, S., Roy, U., Srivastava, A. et al. (2017) Bacterial communities in ancient permafrost profiles of Svalbard, Arctic. *Journal of Basic Microbiology*, 57, 1018–1036.

Tarnocai, C. (1993) Sampling frozen soils. In: Carter, M.R. (Ed.) *Soil sampling and methods of analysis*. Boca Raton, FL: Taylor & Francis, pp. 755–767.

Tarnocai, C., Canadell, J.G., Schuur, E.A.G., Kuhry, P., Mazhitova, G. & Zimov, S. (2009) Soil organic carbon pools in

the northern circumpolar permafrost region. *Global Biogeochemical Cycles*, 23(2), GB2023.

Taş, N., Prestat, E., Wang, S., Wu, Y., Ulrich, C., Kneafsey, T. et al. (2018) Landscape topography structures the soil microbiome in arctic polygonal tundra. *Nature Communications*, 9(777), 1–13.

Team, R.C. (2013) *R: a language and environment for statistical computing*.

Tripathi, B.M., Kim, H.M., Jung, J.Y., Nam, S., Ju, H.T., Kim, M. et al. (2019) Distinct taxonomic and functional profiles of the microbiome associated with different soil horizons of a moist tussock tundra in Alaska. *Frontiers in Microbiology*, 10(1442), 1–14.

Tripathi, B.M., Kim, M., Kim, Y., Byun, E., Yang, J.W., Ahn, J. et al. (2018) Variations in bacterial and archaeal communities along depth profiles of Alaskan soil cores. *Scientific Reports*, 8(1), 1–11.

Tveit, A.T., Urich, T., Frenzei, P. & Svenning, M.M. (2015) Metabolic and trophic interactions modulate methane production by arctic peat microbiota in response to warming. *Proceedings of the National Academy of Sciences of the United States of America*, 112, E2507–E2516.

Varsadiya, M., Urich, T., Hugelius, G. & Barta, J. (2021) Microbiome structure and functional potential in permafrost soils of the Western Canadian Arctic. *FEMS Micobiology Ecology*, 97(3), fiab008.

Waldrop, M.P., Wickland, K.P., White, R., III, Berhe, A.A., Harden, J.W. & Romanovsky, V.E. (2010) Molecular investigations into a globally important carbon pool: permafrost-protected carbon in Alaskan soils. *Global Change Biology*, 16(9), 2543–2554.

Walker, D.A., Hamilton, T.D., Maier, H.A., Munger, C.A. & Raynolds, M.K. (2014) Glacial history and long-term ecology in the Toolik Lake region. In: Hobbie, J.E. & Kling, G.W. (Eds.) *Alaska's changing Arctic: ecological consequences for tundra, streams and lakes*. New York: Oxford University Press, pp. 61–80.

Walker, M.A., Daniëls, F.J. & van der Maarel, E. (1994) Circumpolar arctic vegetation: Introduction and perspectives. *Journal of Vegetation Science*, 5(6), 757–764.

Wallenstein, M.D., McMahon, S. & Schimel, J. (2007) Bacterial and fungal community structure in Arctic tundra tussock and shrub soils. *FEMS Microbiology Ecology*, 59(2), 428–435.

Wilhelm, R.C., Niederberger, T.D., Greer, C. & Whyte, L.G. (2011) Microbial diversity of active layer and permafrost in an acidic wetland from the Canadian high Arctic. *Canadian Journal of Microbiology*, 57, 303–315.

Willerslev, E., Hansen, A.J., Rønn, R., Brand, T.B., Barnes, I., Wiuf, C. et al. (2004) Long-term persistence of bacterial DNA. *Current Biology*, 14, R9–R10.

Williams, P.J. & Smith, M.W. (1989) *The frozen earth: fundamentals of geocryology*. New York: Cambridge University Press.

Wunderlin, T., Junier, T., Roussel-Delif, L., Jeanneret, N. & Junier, P. (2014) Endospore-enriched sequencing approach reveals unprecedented diversity of Firmicutes in sediments. *Environmental Microbiology Reports*, 6, 631–639.

Yergeau, E., Hogues, H., Whyte, L.G. & Greer, C.W. (2010) The functional potential of high Arctic permafrost revealed by metagenomic sequencing, qPCR and microarray analyses. *The ISME Journal*, 4, 1206–1214.

Zak, D.R. & Kling, G.W. (2006) Microbial community composition and function across an arctic tundra landscape. *Ecology*, 87(7), 1659–1670.

SUPPORTING INFORMATION

Additional supporting information can be found online in the Supporting Information section at the end of this article.

How to cite this article: Romanowicz, K.J. & Kling, G.W. (2022) Summer thaw duration is a strong predictor of the soil microbiome and its response to permafrost thaw in arctic tundra. *Environmental Microbiology*, 1–18. Available from: https://doi.org/10.1111/1462-2920.16218

Supplemental Information

Summer thaw duration is a strong predictor of the soil microbiome and its response to permafrost thaw in arctic tundra

Karl J. Romanowicz [1] and George W. Kling [1*]

Affiliations
[1] University of Michigan

*Corresponding Author
Department of Ecology and Evolutionary Biology
University of Michigan
1105 N. University Ave.
Ann Arbor, MI 48109-1085
Phone: 734.647.0894
gwk@umich.edu

This PDF file includes:

Supplemental Methods

Tundra Types. This study investigates soil microbiomes within two tundra types: moist acidic tussock (MAT) tundra and wet sedge (WS) tundra. MAT tundra is dominated by *Eriophorum vaginatum* (tussock-forming sedge) and co-dominated by other graminoids, evergreen and deciduous shrubs, and bryophytes (Walker *et al*., 1994). WS tundra is dominated by sedges (*Carex aquatilis*, *C. chordorrhize, C. rotundata*) (Walker *et al*., 1994). MAT tundra typically forms on ice-rich sediments with a shallow active layer and low soil pH (3.8-5.5 in the Toolik Lake area), whereas WS tundra forms as a rich fen complex with greater active layer thaw depth than upslope MAT tundra (Walker *et al*., 1994).

DNA Extraction and Sequencing. Genomic DNA was extracted in triplicate (0.3-0.4 g soil per replicate) from each 10-cm soil profile increment using the DNeasy PowerSoil DNA Isolation Kit (Qiagen, Germany). A DNeasy PowerClean Pro Cleanup Kit (Qiagen) was used to remove PCR inhibitors from the extracted DNA. DNA was then quantified using the Quant-iT dsDNA High Sensitivity Assay Kit and Qubit 4.0 fluorometer (Invitrogen, USA). DNA was amplified through polymerase chain reaction (PCR) using dual-barcoded primers 515f-806r of the V4 region of the 16S rRNA gene to profile the bacterial and archaeal communities (Apprill *et al*., 2015; Parada *et al*., 2016). Each 16S rRNA reaction contained 10 μL Platinum Hot Start PCR Master Mix (2x) (Thermo Fisher Scientific), 13 μL PCR-grade water, 0.5 μL forward primer (10 μM), 0.5 μL reverse primer (10 μM), and 1 μL template DNA. Amplifications were performed using a Mastercycler ProS thermocycler (Eppendorf, USA). The PCR conditions were: enzyme activation at 94°C for 3 min, followed by 35 cycles of denaturation at 94°C for 45 s, annealing at 50°C for 60 s, and extension at 72°C for 90 s, followed by final extension at 72°C for 10 min. PCR amplicon concentration ranged from 5-30 ng/μL. Dual-barcoded PCR amplicons were pooled into a single library in equal molar concentration (50 ng/amplicon) and submitted to the University of Michigan Microbiome Core for 2×150 bp paired-end high-throughput sequencing on the Illumina MiSeq platform.

Soil Physicochemical Measurements. Soil physicochemical properties were measured from each 10-cm soil profile increment. Soil pH and electrical conductivity (μS cm^{-1}) were measured in a soil:water suspension (1:5 ratio, w/v) using a WTW SenTix pH 3210 meter and probe (resolution: 0.001 pH; Xylem Analytics, Germany) and a WTW Cond 3210 meter and probe (resolution: 0.001 mS/cm; Xylem Analytics), respectively. Soil water content (%) was measured by weighing each sample before and after drying at 105°C for 12 h. Soil organic carbon content (%) was determined from loss on ignition (LOI) analysis by combusting a dried subsample at 550°C for 8 h, assuming the mass of organic matter lost during ignition was ~36% carbon for organic soils and ~7% carbon for mineral soils (G. Kling, unpublished).

Caldisericota Annotations. The soil microbiomes in this study contain taxonomic annotations attributed to the phylum Caldisericota (order Caldisericales; Fig. 3; Table 2). Caldisericota is also reported in numerous arctic studies (Monteux *et al*., 2018; Tas *et al*., 2018; Tripathi *et al*., 2018; 2019, Varsadiya *et al*., 2021). However, this taxonomic annotation in tundra soils is likely misleading due to recent taxonomic revisions. Caldisericota is a known hot spring sulfur-reducing chemoheterotroph within the 16S rRNA gene lineage 'OP5' and named for the sole isolate *Caldisericum exile* (Hugenholtz *et al*., 1998). In Martinez *et al*. (2019), seven Caldisericota

metagenome-assembled genomes (MAGs) were characterized from a thawing permafrost site in arctic Sweden and proposed to form a divergent clade from *C. exile* at the phylum level. These permafrost Caldisericota, now proposed as *Candidatus* Cryosericota phylum, were characterized as carbohydrate and amino acid fermenters capable of using labile plant compounds and peptides while also encoded with adaptations to low temperatures (Martinez *et al*., 2019). Future studies should recognize this discrepancy in taxonomic annotations based on currently available 16S rRNA gene databases.

Bacterial Cell Viability Assays. Bacterial cells were separated from the soil matrix of select 10-cm soil profile increment using Nycodenz density cushion centrifugation following methods from Burkert *et al*. (2019). Three 10-cm soil increment depths were selected from each soil profile to represent a surface active-layer depth (~10-20 cm), a transition zone depth (~40-50 cm), and a permafrost depth (~70-80 cm). To separate cells from soil debris, 5 g of soil was disrupted in 5 mL of a mild detergent consisting of 0.5% Tween 80 (Thermo Fisher Scientific) and 50 mM sodium pyrophosphate buffer (Alfa Aesar, USA) and vortexed for 15 min. Vortexed samples were centrifuged at 750 x g for 7 minutes at 4°C to remove large particles and debris. The supernatant (600 µL) was extracted and layered over 600 µL of 1.3 g/L Nycodenz (Cosmo Bio, USA) solution in a 2-mL tube. Tubes were centrifuged at 14,000 x g for 30 min at 4°C. The upper and middle phases (600 µL) containing bacterial cells were transferred into a sterile 2-mL tube and centrifuged at 10,000 x g for 15 min at 4°C. The supernatant was discarded, and the pellet was resuspended in 1 mL of 0.85% NaCl solution. The viability assay was performed with a Live/Dead BacLight Bacterial Viability Kit (Invitrogen) per manufacturer instructions. The stained cell suspensions were filtered onto a 25-mm-diameter 0.2-µm-pore-size black polycarbonate membrane and placed on a slide with sterile forceps. Images were captured at 60x total magnification (Nikon Eclipe T*i* confocal microscope). Viable cells (green fluorescence) and dead cells (red fluorescence) were counted using Imaris post-processing software (Oxford Instruments Group); and a consistent field of view (~62×212 µm area) was counted for live- and dead-stained cells. The average number of cells per field of view was multiplied by area of the filter, and the dilution factor was then corrected for dry weight to calculate the average number of cells per gram of soil dry weight (g dw^{-1}).

Thaw Depth Measurements. Annual thaw depth measurements began in 1990 at a small watershed just south of Toolik Lake, and in 2002 in the Imnavait Creek basin. Thaw depth at each of 96 sites at Toolik and 75 sites at Imnavait was measured each year on 2 July and 11 August (plus or minus 1 day). UTM stakes every 100 m define the grids, and measurements were made every 25 m in between the UTM stakes. Survey grids at both sites cover a gently sloping hill of MAT tundra dominated by *E. vaginatum*, and at Imnavait the grid extends into WS tundra in the valley bottom and in the riparian zone of the creek. Within a 100 cm radius of each grid point, a ruled stainless-steel rod was inserted in inter-tussock microhabitat (the space between tussocks) until the frozen layer was reached, and the distance was measured to the top of the upper soil organic mat (beneath the uppermost moss layer if present). Two measurements were made at each point from 1990-1999, and three measurements were made at each point from 2000 on. The measurements for all sites on the grid were averaged to arrive at a single number (plus a standard error) for each date in each year. Variability in annual thaw progression is shown in Figure S3.

References

Apprill, A., McNally, S., Parsons, R., and Weber, L. (2015) Minor revision to V4 region SSU rRNA 806R gene primer greatly increases detection of SAR11 bacterioplankton. *Aquatic Microbial Ecology* **75(2)**: 129-137.

Burkert, A., Douglas, T.A., Waldrop, M.P., and Mackelprang, R. (2019) Changes in the active, dead, and dormant microbial community structure across a Pleistocene permafrost chronosequence. *Appl Environ Microbiol* **85(7)**: e02646-18.

Hugenholtz, P., Pitulle, C., Hershberger, K.L., and Pace, N.R. (1998) Novel division level bacterial diversity in a Yellowstone hot spring. *J Bacteriol* **180**: 366–376.

Martinez, M.A., Woodcroft, B.J., Ignacio Espinoza, J.C., *et al*. (2019) Discovery and ecogenomic context of a global Caldiserica-related phylum active in thawing permafrost, Candidatus Cryosericota phylum nov., Ca. Cryosericia class nov., Ca. Cryosericales ord. nov., Ca. Cryosericaceae fam. nov., comprising the four species Cryosericum septentrionale gen. nov. sp. nov., Ca. C. hinesii sp. nov., Ca. C. odellii sp. nov., Ca. C. terrychapinii sp. nov. *Systematic and Applied Microbiology* **42**: 54-66.

Monteux, S., Weedon, J.T., Blume-Werry, G., *et al*. (2018) Long-term in situ permafrost thaw effects on bacterial communities and potential aerobic respiration. *ISME J* **12**: 2129-2141.

Parada, A.E., Needham, D.M., and Fuhrman, J.A. (2016) Every base matters: assessing small subunit rRNA primers for marine microbiomes with mock communities, time series and global field samples. *Environmental Microbiology* **18(5)**: 1403-1414.

Taş, N., Prestat, E., Wang, S., *et al*. (2018) Landscape topography structures the soil microbiome in arctic polygonal tundra. *Nature Communications* **9(777)**: 1-13.

Team, R.C. (2018) R: A language and environment for statistical computing.

Tripathi, B.M., Kim, M., Kim, Y., *et al*. (2018) Variations in bacterial and archaeal communities along depth profiles of Alaskan soil cores. *Scientific Reports* **8(1)**: 1-11.

Tripathi, B.M., Kim, H.M., Jung, J.Y., *et al*. (2019) Distinct taxonomic and functional profiles of the microbiome associated with different soil horizons of a moist tussock tundra in Alaska. *Frontiers in Microbiology* **10(1442)**: 1-14.

Varsadiya, M., Urich, T., Hugelius, G., and Barta, J. (2021) Microbiome structure and functional potential in permafrost soils of the Western Canadian Arctic. *FEMS Micobiology Ecology* **97(3)**: fiab008.

Walker, M.A., Daniëls, F.J., and van der Maarel, E. (1994) Circumpolar arctic vegetation: Introduction and perspectives. *Journal of Vegetation Science* **5(6)**: 757-764.

Supplemental Tables

Table S1. Physicochemical properties of soils from Toolik (youngest landscape age), Imnavait (intermediate landscape age), and Sagwon (oldest landscape age) sampling sites (mean ± SD) measured from soil profile samples. Letters indicate significant differences between each site × tundra type interaction (ANOVA; $p < 0.05$).

	Toolik Lake		Imnavait Creek		Sagwon Hills	
Soil Property	**MAT Tundra**	**WS Tundra**	**MAT Tundra**	**WS Tundra**	**MAT Tundra**	**WS Tundra**
Soil pH	5.0 ± 0.5 [a]	5.3 ± 0.3 [a]	5.3 ± 0.4 [a]	4.6 ± 0.3 [b]	6.2 ± 0.4 [c]	5.7 ± 0.2 [a,c]
Conductivity (µS/cm)	30.7 ± 26.9 [a]	18.6 ± 10.0 [a]	22.1 ± 23.5 [a]	22.9 ± 13.7 [a]	84.5 ± 73.4 [b]	52.7 ± 28.5 [a,b]
Water Content (%)	58.7 ± 22.8 [a]	81.2 ± 4.1 [b]	42.4 ± 27.5 [a]	76.7 ± 5.5 [b]	49.7 ± 14.1 [a]	81.8 ± 6.9 [b]
Organic C (%)	7.4 ± 11.7 [a]	24.0 ± 1.4 [b]	7.6 ± 12.9 [a]	21.7 ± 2.9 [b]	4.8 ± 7.1 [a]	30.1 ± 2.2 [b]

Table S2. Bacterial cell viability assay results. Viable cells (green fluorescence) and dead cells (red fluorescence) were counted from a consistent field of view (~62×212 μm area). The average number of cells per field of view was multiplied by the area of the filter (25 μm diameter) and the dilution factor was then corrected for dry weight to calculate the average number of cells per gram of soil (g dw^{-1}).

Site	Soil Type	Live Cells (g dw^{-1})	Dead Cells (g dw^{-1})	Total Cells (g dw^{-1})	% Live	% Dead
Toolik Lake						
MAT Tundra						
10-20 cm	Organic	1.7E+07	8.8E+06	2.6E+07	66	34
40-50 cm	Mineral	1.0E+07	1.5E+07	2.5E+07	41	59
70-80 cm	Mineral	2.6E+07	1.4E+07	4.0E+07	64	36
WS Tundra						
10-20 cm	Organic	1.8E+08	6.6E+07	2.5E+08	73	27
40-50 cm	Organic	1.1E+08	7.5E+07	1.8E+08	59	41
70-80 cm	Organic	5.8E+07	1.0E+08	1.6E+08	36	64
Imnavait Creek						
MAT Tundra						
10-20 cm	Organic	2.8E+06	4.7E+06	7.5E+06	37	63
40-50 cm	Mineral	1.3E+07	1.4E+07	2.6E+07	48	52
60-70 cm	Mineral	1.8E+06	2.7E+06	4.5E+06	40	60
WS Tundra						
10-20 cm	Organic	7.0E+07	7.2E+07	1.4E+08	49	51
50-60 cm	Organic	3.6E+07	2.8E+07	6.4E+07	56	44
80-90 cm	Organic	5.8E+07	2.5E+07	8.3E+07	70	30
Sagwon Hills						
MAT Tundra						
10-20 cm	Organic	6.7E+06	4.0E+06	1.1E+07	63	37
40-50 cm	Mineral	2.8E+07	3.4E+07	6.2E+07	45	55
70-80 cm	Mineral	3.3E+07	6.4E+06	3.9E+07	84	16
WS Tundra						
10-20 cm	Organic	6.2E+07	2.3E+07	8.5E+07	73	27
50-60 cm	Organic	1.1E+07	6.1E+06	1.7E+07	65	35
60-70 cm	Organic	3.2E+07	1.8E+07	5.0E+07	64	36

Table S3. Summary statistics for 16S rRNA amplicon sequencing reads (N = 51). Total reads for all samples were rarified to 50,487 based on the sample with lowest final QC read count (bold).

Sampling Location	Soil Depth (cm)	Sample Soil Type	Total Reads	QC Reads	Read % Passed QC	Denoised Reads	Merged Reads	Final QC Reads	Rarified Reads
Toolik MAT	0-10	Organic	145,893	135,011	92.5	131,009	112,610	99,213	50,487
Toolik MAT	10-20	Organic	143,621	132,327	92.1	130,652	118,987	113,108	50,487
Toolik MAT	20-30	Mineral	169,491	151,159	89.2	146,057	124,271	121,265	50,487
Toolik MAT	30-40	Mineral	144,516	126,819	87.8	122,281	101,393	98,581	50,487
Toolik MAT	40-50	Mineral	146,451	134,160	91.6	131,365	113,036	108,298	50,487
Toolik MAT	50-60	Mineral	150,291	136,413	90.8	134,033	119,080	116,510	50,487
Toolik MAT	60-70	Mineral	176,030	152,387	86.6	150,640	130,358	128,078	50,487
Toolik MAT	70-80	Mineral	140,707	127,591	90.7	125,232	113,744	112,623	50,487
Toolik MAT	80-90	Mineral	153,994	141,790	92.1	140,000	124,463	121,874	50,487
Toolik WS	0-10	Organic	152,304	138,741	91.1	133,977	118,540	114,110	50,487
Toolik WS	10-20	Organic	141,525	131,406	92.9	128,807	117,276	113,976	50,487
Toolik WS	20-30	Organic	179,751	165,089	91.8	160,086	143,047	138,967	50,487
Toolik WS	30-40	Organic	152,433	140,317	92.1	136,556	121,025	117,963	50,487
Toolik WS	40-50	Organic	128,652	119,347	92.8	118,859	109,161	108,166	50,487
Toolik WS	50-60	Organic	136,304	126,031	92.5	123,227	101,279	97,039	50,487
Toolik WS	**60-70**	**Organic**	**71,984**	**62,605**	**87.0**	**62,413**	**50,912**	**50,487**	**50,487**
Toolik WS	70-80	Organic	160,557	148,465	92.5	147,072	127,336	126,111	50,487
Toolik WS	80-90	Organic	184,135	171,370	93.1	169,908	150,769	148,565	50,487
Imnavait MAT	0-10	Organic	186,102	173,532	93.3	169,139	157,394	147,867	50,487
Imnavait MAT	10-20	Organic	183,512	170,117	92.7	165,179	143,596	134,175	50,487
Imnavait MAT	20-30	Mineral	198,388	179,830	90.7	175,505	158,690	149,953	50,487
Imnavait MAT	30-40	Mineral	166,394	149,995	90.1	147,659	133,360	130,345	50,487
Imnavait MAT	40-50	Mineral	205,995	190,971	92.7	188,847	170,584	167,215	50,487
Imnavait MAT	50-60	Mineral	194,935	180,092	92.4	178,448	155,989	154,251	50,487
Imnavait MAT	60-70	Mineral	213,609	188,730	88.4	187,380	165,323	164,634	50,487
Imnavait WS	0-10	Organic	172,255	157,020	91.2	150,094	132,458	124,259	50,487
Imnavait WS	10-20	Organic	159,528	147,334	92.4	146,228	136,053	132,874	50,487
Imnavait WS	20-30	Organic	205,779	190,252	92.5	185,419	163,696	158,643	50,487
Imnavait WS	30-40	Organic	132,079	121,675	92.1	118,549	104,426	102,155	50,487
Imnavait WS	40-50	Organic	159,637	148,434	93.0	144,638	127,701	122,224	50,487
Imnavait WS	50-60	Organic	129,215	118,911	92.0	115,954	101,657	98,961	50,487
Imnavait WS	60-70	Organic	161,786	141,231	87.3	138,077	114,718	112,325	50,487
Imnavait WS	70-80	Organic	147,401	135,626	92.0	133,684	116,765	115,817	50,487
Imnavait WS	80-90	Organic	156,850	144,366	92.0	142,755	115,801	113,187	50,487
Imnavait WS	90-100	Organic	139,103	128,207	92.2	125,823	112,836	112,077	50,487
Sagwon MAT	0-10	Organic	120,233	109,426	91.0	102,474	88,650	82,863	50,487
Sagwon MAT	10-20	Organic	130,657	119,780	91.7	113,138	96,670	94,001	50,487
Sagwon MAT	20-30	Organic	166,257	150,804	90.7	143,036	121,729	116,872	50,487
Sagwon MAT	30-40	Mineral	139,421	125,087	89.7	119,247	102,321	100,522	50,487
Sagwon MAT	40-50	Mineral	153,499	140,181	91.3	135,239	123,478	120,791	50,487
Sagwon MAT	50-60	Mineral	167,262	151,569	90.6	145,773	127,358	123,316	50,487
Sagwon MAT	60-70	Mineral	151,468	128,319	84.7	122,868	108,215	106,018	50,487
Sagwon MAT	70-80	Mineral	127,396	116,182	91.2	112,492	103,903	101,149	50,487
Sagwon MAT	80-90	Mineral	135,695	125,971	92.8	123,849	117,819	114,960	50,487
Sagwon WS	0-10	Organic	126,143	115,402	91.5	112,160	98,963	89,976	50,487
Sagwon WS	10-20	Organic	110,165	100,463	91.2	97,246	87,927	84,537	50,487
Sagwon WS	20-30	Organic	141,939	125,340	88.3	121,654	109,385	106,669	50,487
Sagwon WS	30-40	Organic	130,151	115,488	88.7	111,840	104,865	102,734	50,487
Sagwon WS	40-50	Organic	138,530	127,706	92.2	125,464	107,666	105,685	50,487
Sagwon WS	50-60	Organic	153,001	140,276	91.7	137,451	117,805	116,016	50,487
Sagwon WS	60-70	Organic	150,502	129,839	86.3	126,092	104,483	101,975	50,487

Supplemental Figures

Figure S1. Box plots for Chao1 (**A**) and Shannon (**B**) alpha diversity and Bray-Curtis (**C**) beta diversity based on the abundance of amplicon sequence variants (ASVs) at each sampling location. Asterisks indicate the significance of the differences in mean ASV abundance between sampling locations (ANOVA; *** $p < 0.001$; ** $p < 0.01$; * $p < 0.05$).

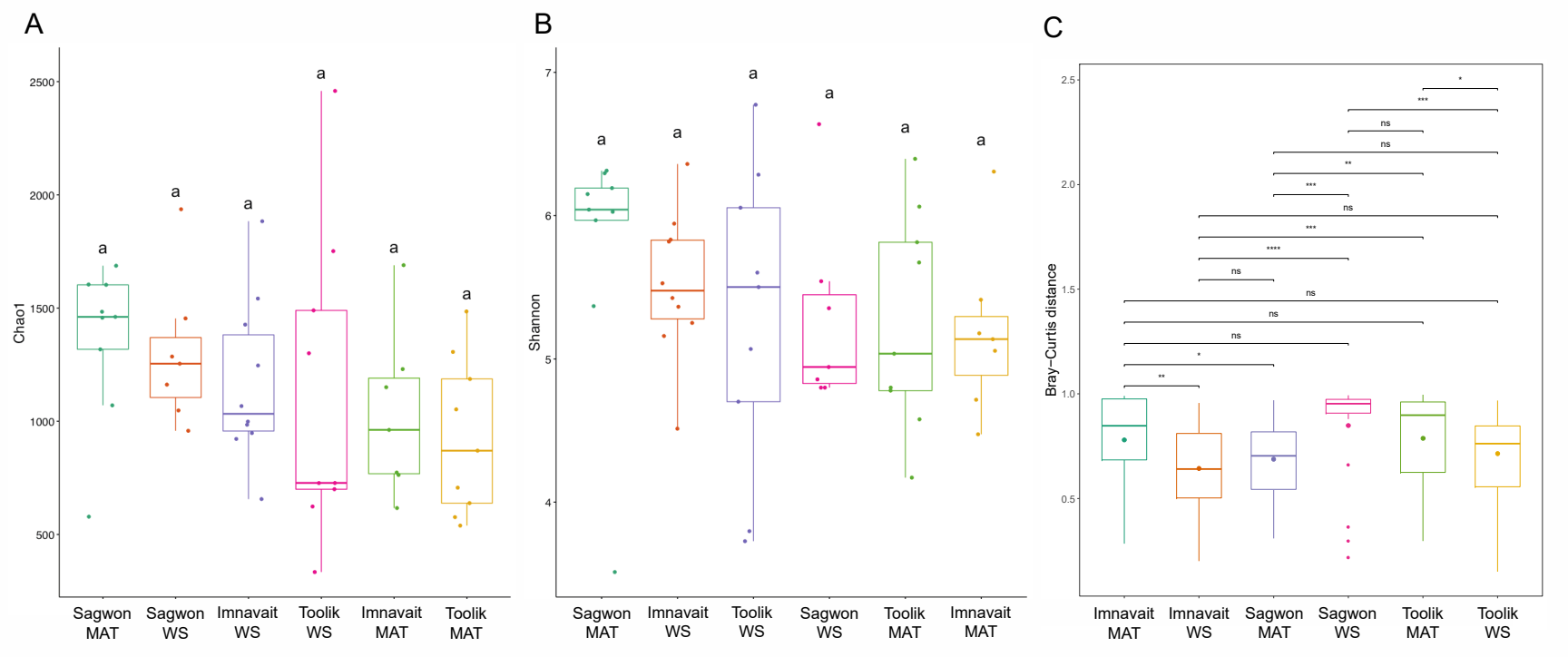

Figure S2. Relative abundance of archaea by depth for each sampling location.

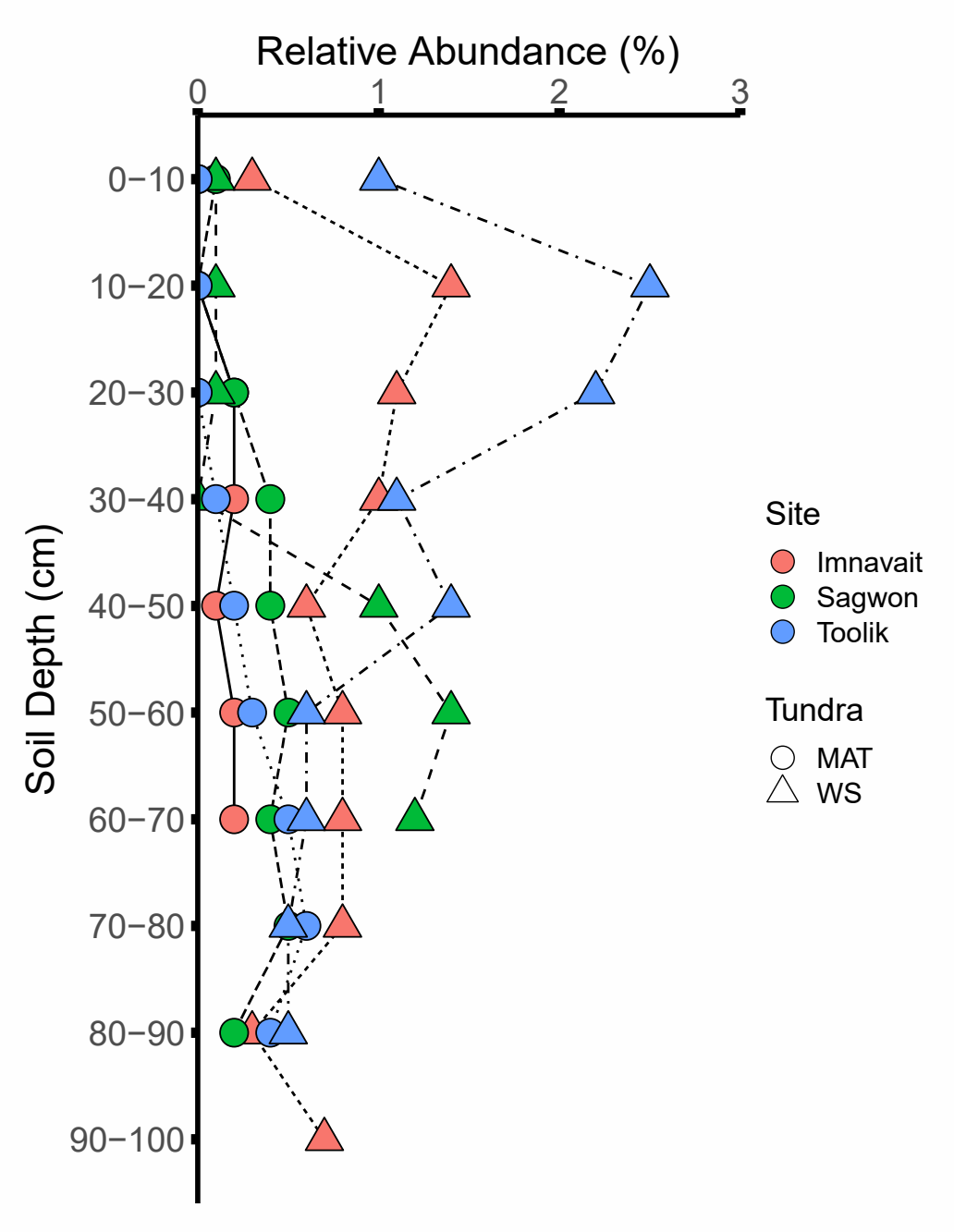

Figure S3. Variability in seasonal thaw at the Imnavait Creek watershed in years 2018-2021, showing that maximum thaw depth at this site occurs in mid-August to early September. Because the soil profile study was conducting in 2018, we have retained only those thaw duration values that correspond with the sequencing dataset for all downstream analyses presented in the manuscript. Data points and standard error bars were generated as described in the Supplemental Information text under "Thaw Depth Measurements".